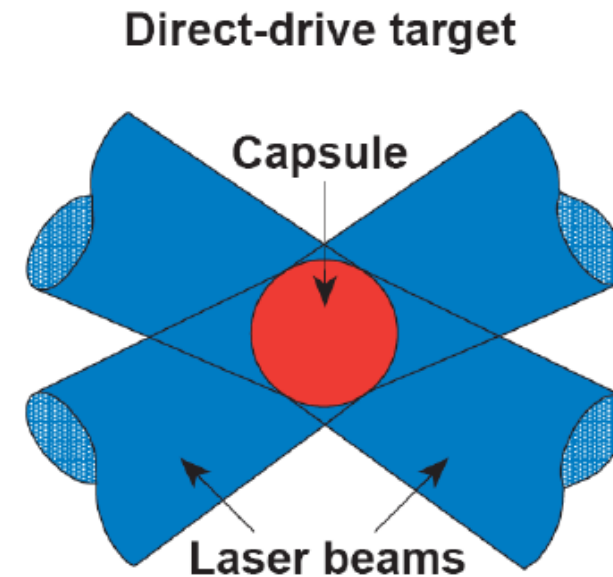
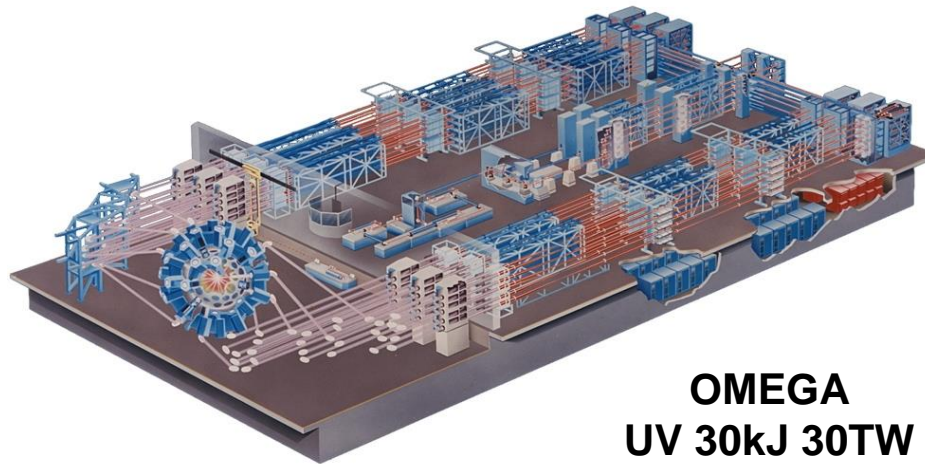


Progress in Laser Direct-Drive Inertial Confinement Fusion



R. Betti
Chief Scientist, Laboratory for Laser Energetics
Dept. Mechanical Engineering and Physics & Astronomy
University of Rochester

Nuclear Photonics Conference
Durham, NC
September 11-15, 2023

Collaborators



V. Gopaldaswamy, A. Lees, J. Knauer, L. Ceurvorst, D. Patel, R. Ejaz, C. Williams, K.M. Woo, P. Farmakis, D. Cao, C. Thomas, I. Igumenshchev, K. Anderson, T. Collins, R. Epstein, A. Solodov, M. Rosenberg, C. Forrest, C. Stoeckl, R. Shah, V. Glebov, V. Goncharov, D. Turnbull, K. Churnetski, D. Froula, S. Regan, H. McCLOW,

R. Janezic, C. Fella, M. Koch, W. Shmayda and the cryogenics group
M. Bonino, D. Harding and the target fab group
S. Sampat, K.A. Bauer and the System Science group
S. Morse and the OMEGA facility crew

Laboratory for Laser Energetics

M. Gatu Johnson, C. Wink, R.D. Petrasso, CK Li, J.A. Frenje

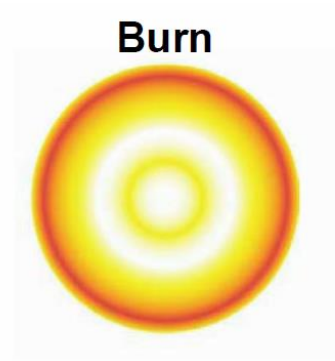
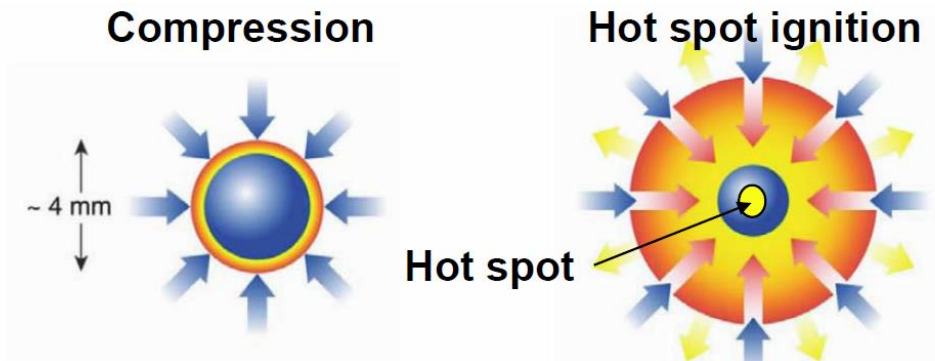
Massachusetts Institute of Technology

C. Shulberg and M. Farrell

General Atomics

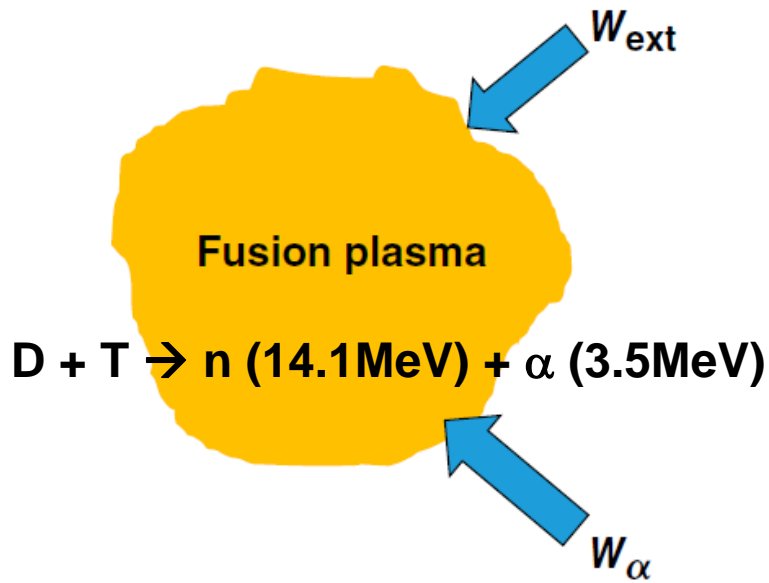
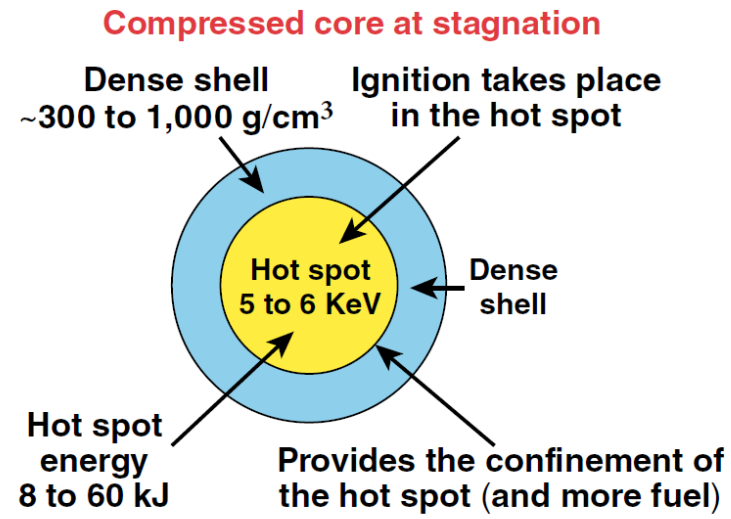
Introduction and implosion designs

Both direct and indirect drive ICF aim to achieve the conditions for thermonuclear ignition and propagating burn



$$Q_{\alpha} \equiv \frac{W_{\alpha}}{W_{\text{ext}}}$$

In ICF $W_{\text{ext}} = W_{\text{pdV}}$



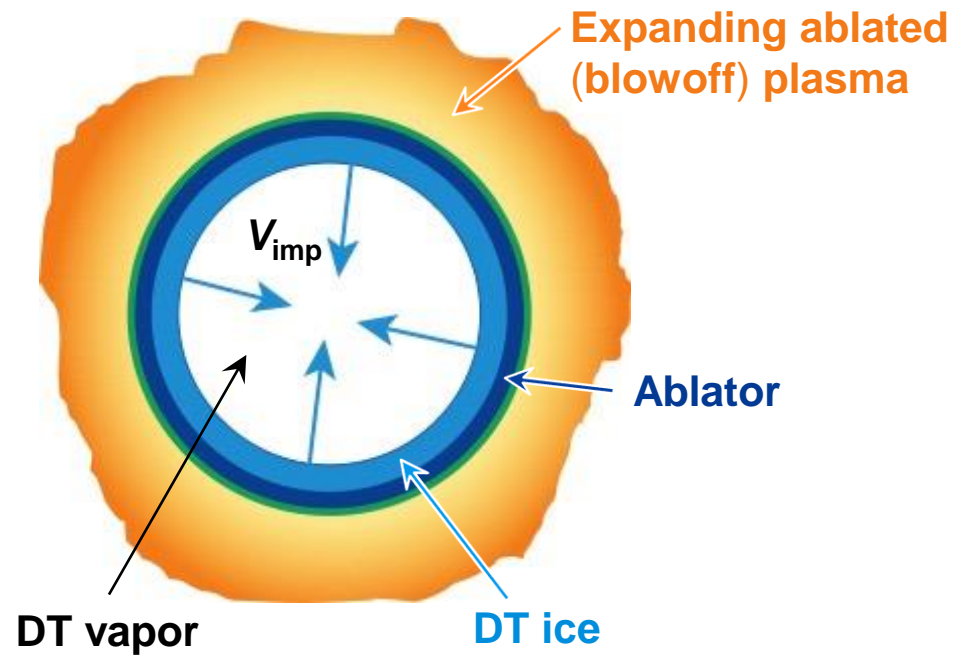
Burning plasmas

$Q_{\alpha} > 1$

Ignited plasmas

$Q_{\alpha} \gg 1$

Driving ICF targets with lasers is a very inefficient process. Direct drive couples more energy to the target than indirect drive



Examples:

Indirect Drive

Laser energy = 2 MJ
Shell final kinetic energy = 20-30 kJ
Total efficiency = 1-1.5%

Direct Drive

Laser energy = 2 MJ
Shell final kinetic energy = 80-100 kJ
Total efficiency = 4-5%

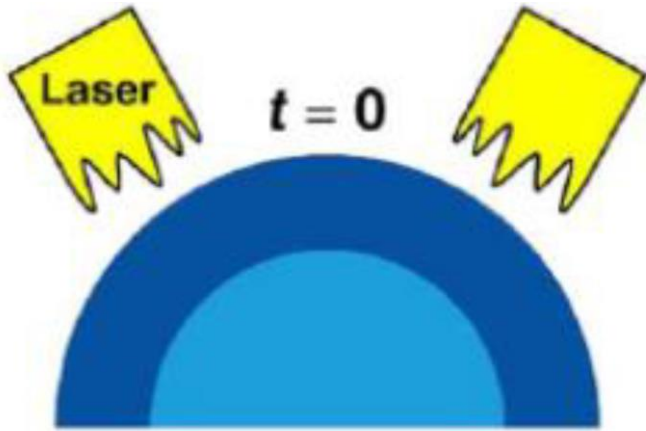
$$\text{Useful kinetic energy} = \frac{1}{2} M_{\text{unablated}}^{\text{shell}} V_{\text{imp}}^2$$

The favorable energetics implies that direct drive can potentially implode larger capsules containing more fuel thus leading to higher fusion yields and higher energy gains than indirect drive

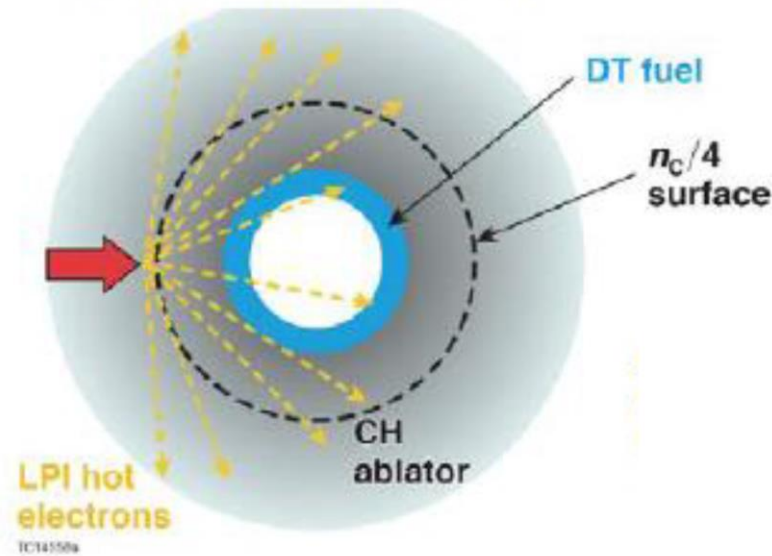
V_{imp} = implosion velocity

Depending on the design, direct-drive implosions are degraded by hydrodynamic and laser-plasma instabilities

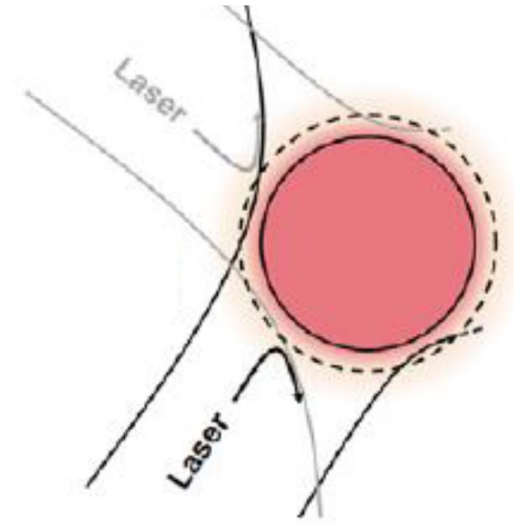
Laser imprinting seeds the Rayleigh-Taylor Instability



Hot electrons from Two-Plasmon Decay and Stimulated Raman Scattering preheat the target in-flight



Cross-Beam Energy Transfer reduces laser energy absorption



Hydro-stability metrics →

The adiabat is mostly set by the strength of the first shock

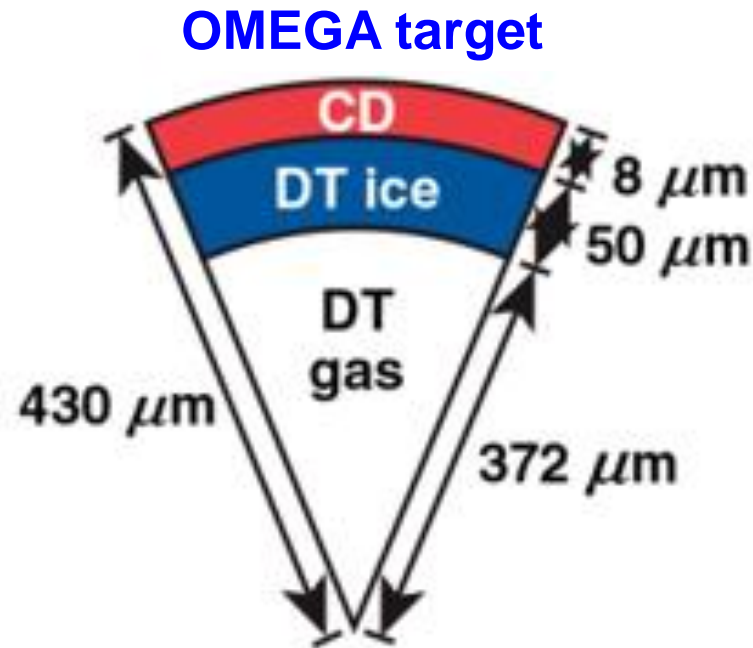
$$adiabat = \alpha_F \equiv \frac{P}{P_{Fermi}}$$

Higher $\alpha_F \rightarrow$ more stable

$$IFAR \equiv \frac{Radius}{Thickness}$$

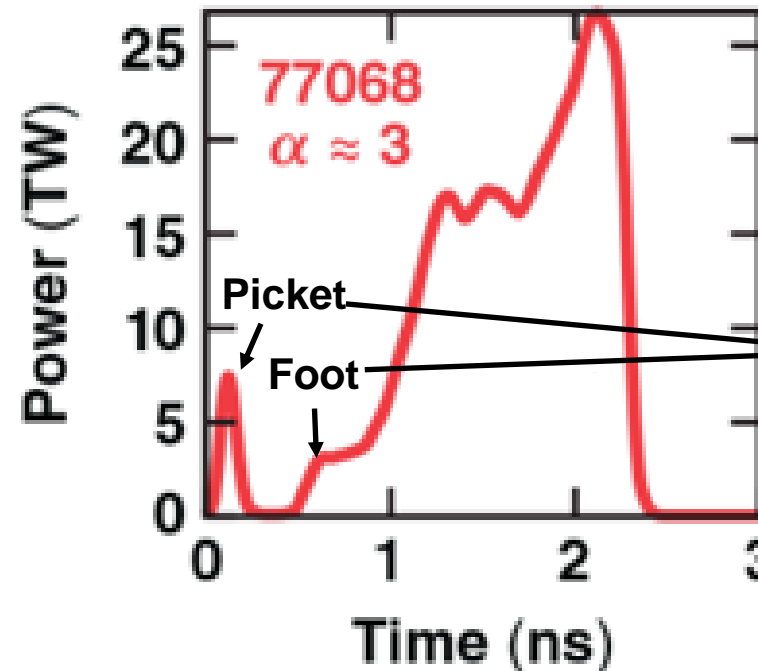
Higher IFAR \rightarrow more unstable

Designing implosions requires achieving an optimal balance between 1D performance and 3D hydro-stability while controlling LPI



Laser pulse shape

Hydro stability Energetics +LPI



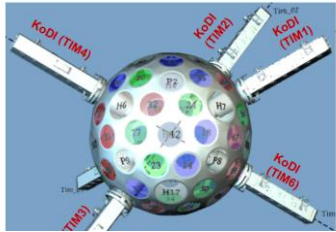
Shocks are launched.
Stronger shock \rightarrow higher adiabat
Adiabat is set
Stability properties are set

Low adiabat is good for 1D convergence/compression while high adiabat is good for 3D stability. Target specs and laser pulse shapes are the knobs we can turn for optimizing implosions

Fusion yield, burn duration, core size, pressure, density, temperature and areal density are the properties measured in implosion experiments

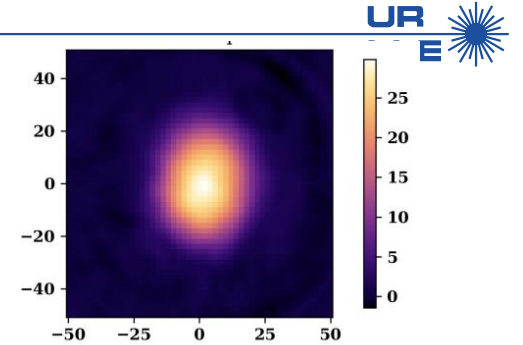
Inference of the core pressure and density

NTOF
+
Activation



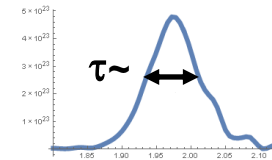
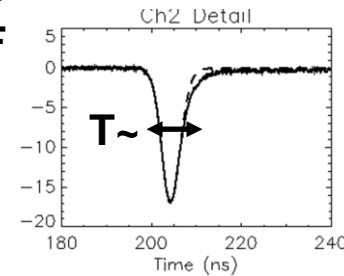
$$\text{Yield} \sim n_{\text{HS}}^2 \langle \sigma v \rangle V \tau \sim P_{\text{HS}}^2 \frac{\langle \sigma v \rangle}{T^2} V \tau$$

x ray

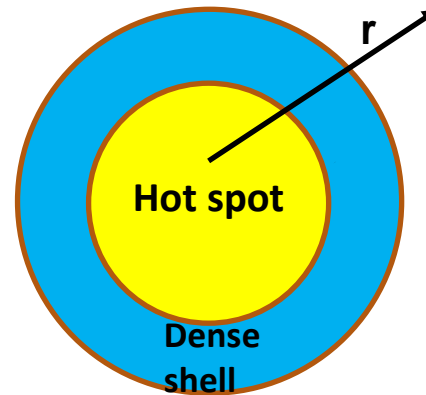
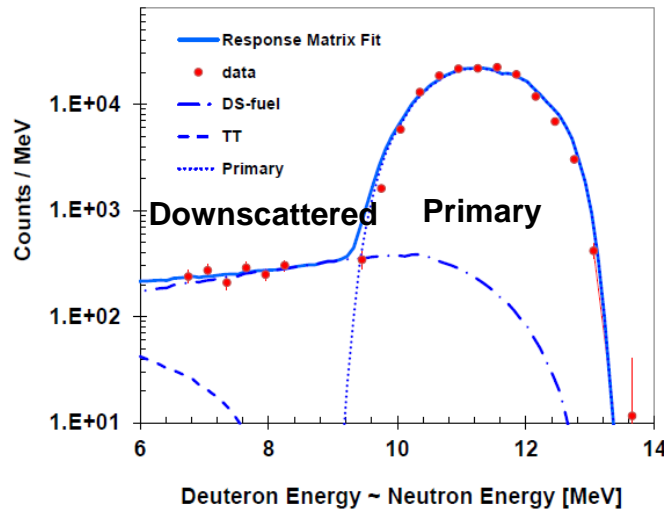


Neutron temporal diagnostic

NTOF
Brisk



Inference of the areal density



$$\rho R = \int_0^{\infty} \rho dr \sim \frac{\text{Downscattered}^1}{\text{Primary}} \sim \frac{\text{Backscattered}^2}{\text{Primary}}$$

- [1] J. Frenje et al, *Rev. Sci. Instrum.* 72(1), 854–858 (2001)
 [2] C. Forrest et al, *Rev. Sci. Instrum.* 83, 10D919 (2012)

A major goal of LLE is to produce scaled ignition conditions on OMEGA for direct drive

- The measurable normalized ignition condition is determined by the Lawson parameter of the compressed core¹⁻⁴

$$\chi_{\text{exp}} = \frac{nT\tau}{[nT\tau]_{\text{ign}}} \sim \left[(\rho R)^2 \left(\frac{Y_{DT}}{M_{DT}} \right) \right]^{1/3}$$

Areal density (MRS, NTOF)
Neutron yield (NTOF+ Cu-activation)
↓
↓
(ρR)
 $\left(\frac{Y_{DT}}{M_{DT}} \right)$
↑ Stagnating DT mass (inferred)

- When scaled hydrodynamically, the Lawson parameter increases linearly with size

$$\chi \sim P\tau \sim \frac{P}{V_{\text{imp}}} R \sim R \qquad E_L \sim V \sim R^3 \Rightarrow R \sim E_L^{1/3}$$

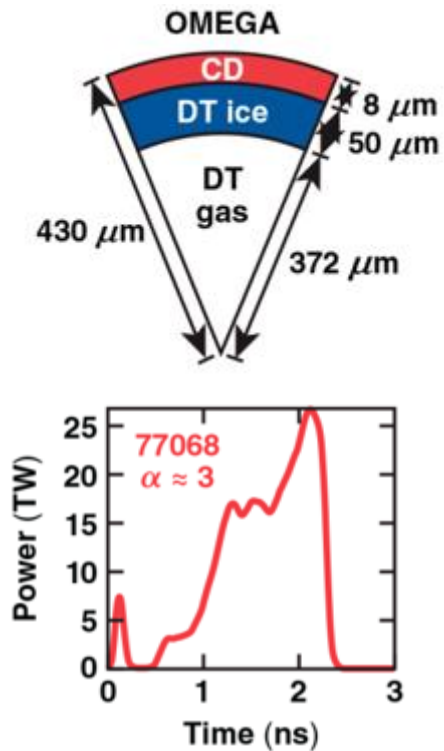
- Hydro-equivalent Ignition condition $\rightarrow \chi_{MJ} \equiv \chi_{\text{OMEGA}} \left(\frac{E_L(\text{MJ})}{E_{\text{Laser}}^{\text{OMEGA}}} \right)^{1/3} \geq 1$

- Hydro-equivalent Burning-Plasma condition² $\rightarrow \chi_{MJ} \geq 0.8$

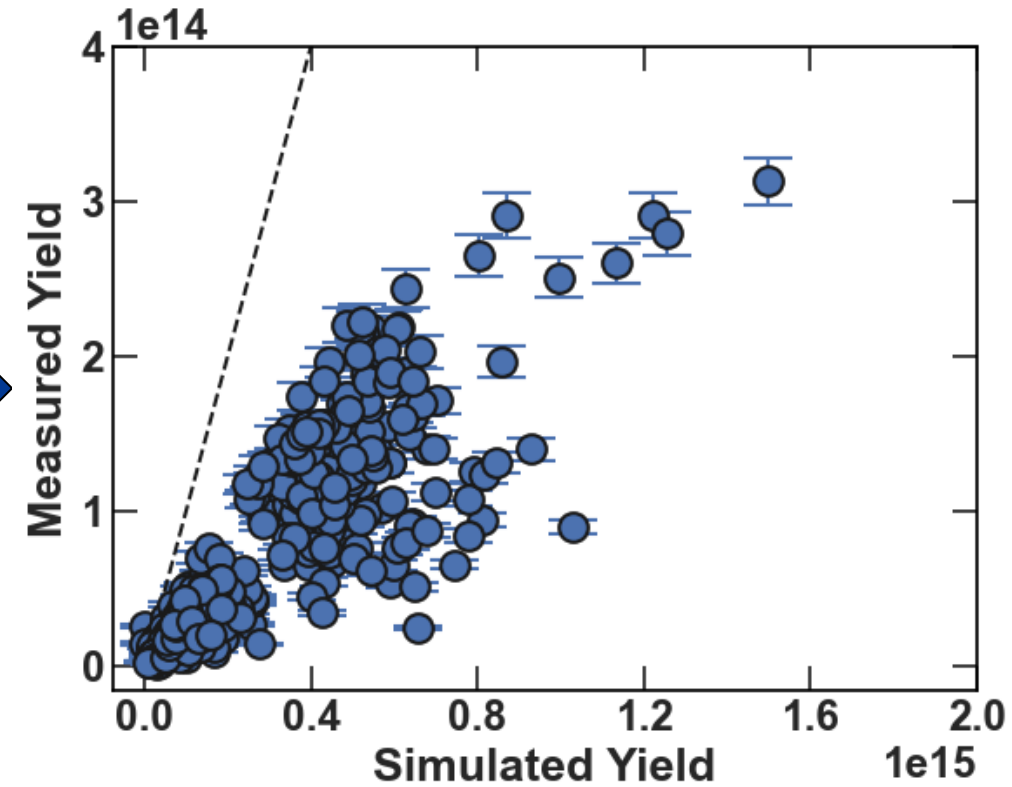
[1] A. Christopherson et al, Phys. Plasmas 27, (2020)
 [2] R. Betti et al, Phys. Rev. Lett. 114, 255003 (2015)
 [3] J. D. Lindl et al. Phys. Plasmas 25, 122704 (2018)
 [4] B.K. Spears et al, Phys. Plasmas 19, 056316 (2012)

Conventional implosion designs use 1-D simulations, which are not accurate enough to guide designs towards optima

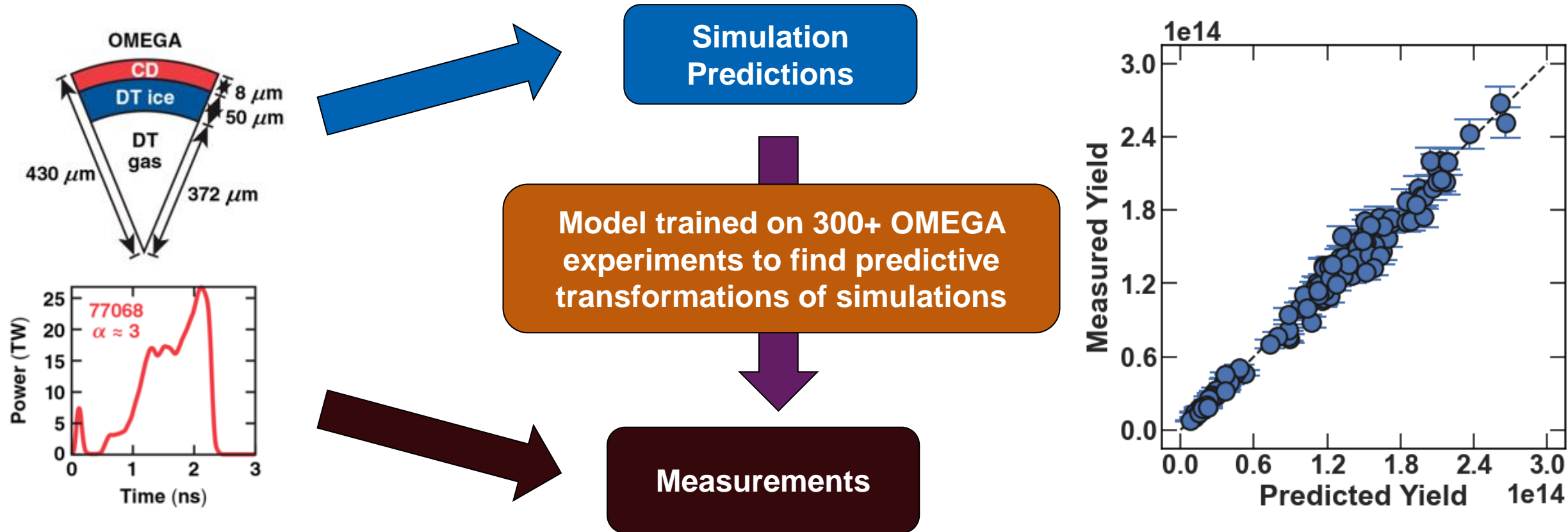
Initial Conditions



Simulations



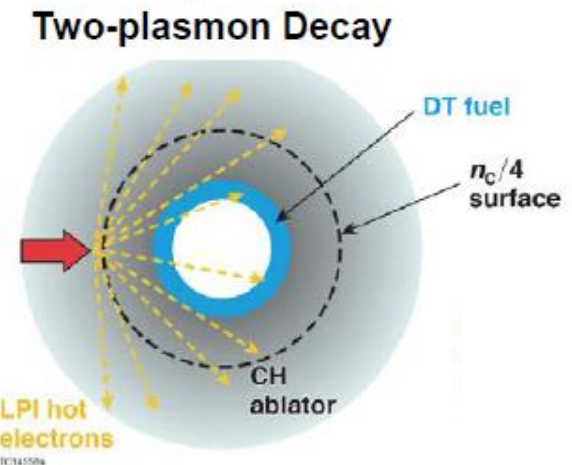
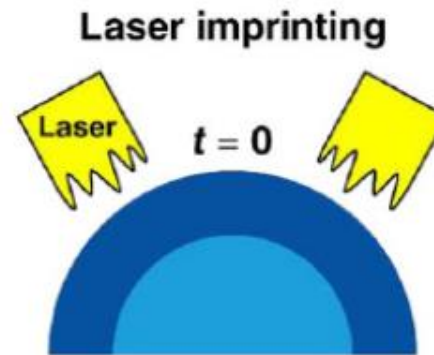
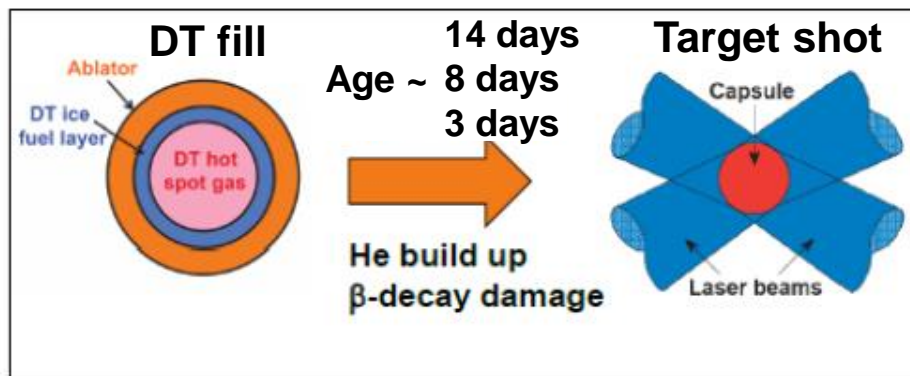
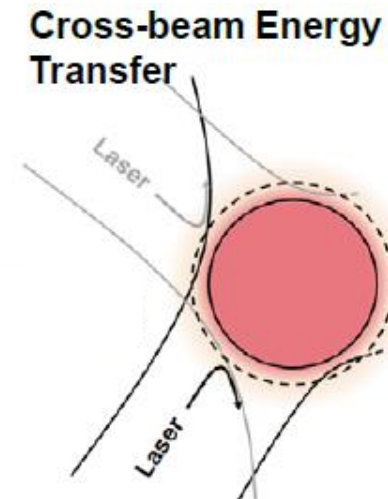
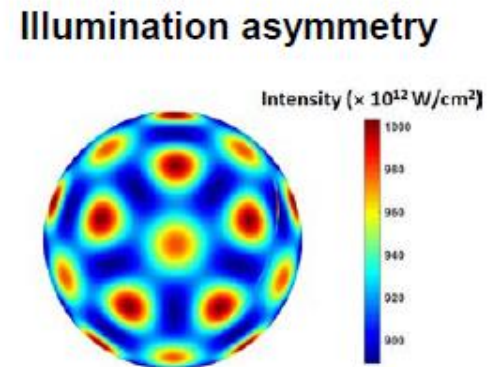
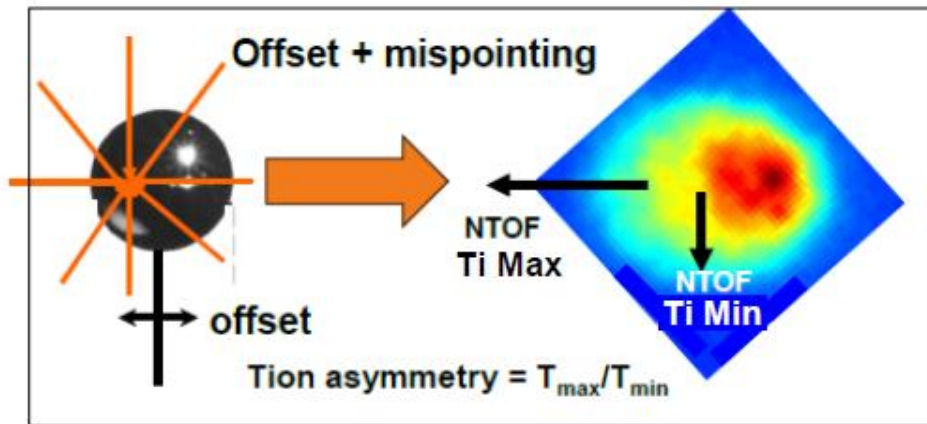
LLE uses a data-driven statistical model (SM) to design high performance implosions



The model is accurate across a wide range of adiabats, convergence ratios, velocities and intensities

- [1] V. Gopaldaswamy et al, Nature 565, 581-586 (2019)
- [2] A. Lees et al, Phys. Rev. Lett. 127, 105001 (2021)
- [3] V. Gopaldaswamy et al, PoP (2021)
- [4] A. Lees et al, PoP (2023)

Many factors impact the performance of direct-drive implosions. The statistical predictions account for all these factors

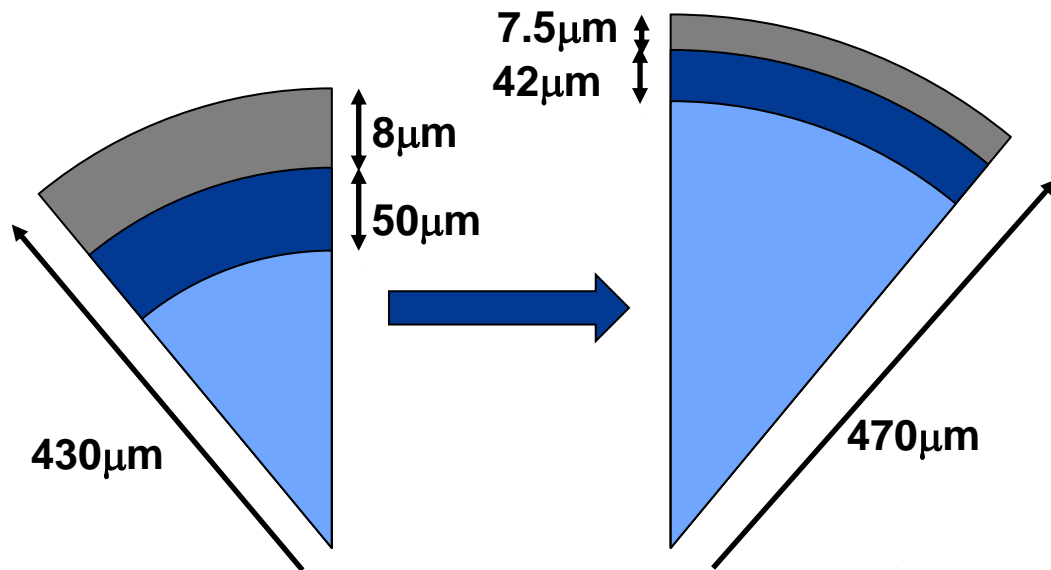


T_i = apparent ion temperature measured by NTOF detectors

Laser pulse shape and target size were modified using statistical predictions. Age of the DT fill (fill-to-shot time) was reduced to three days

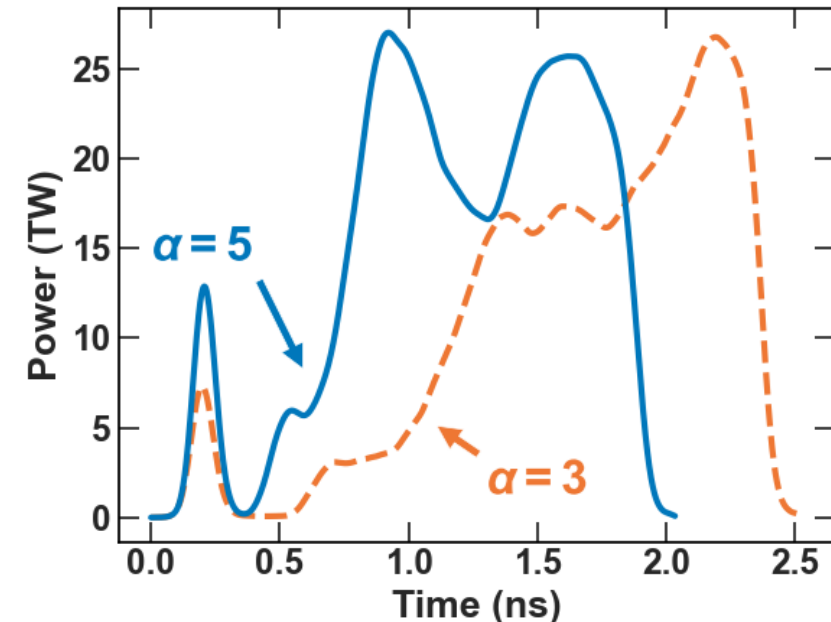
Targets have become

- larger (CBET mitigation)
- thinner ice (faster)



Pulse shape changes include:

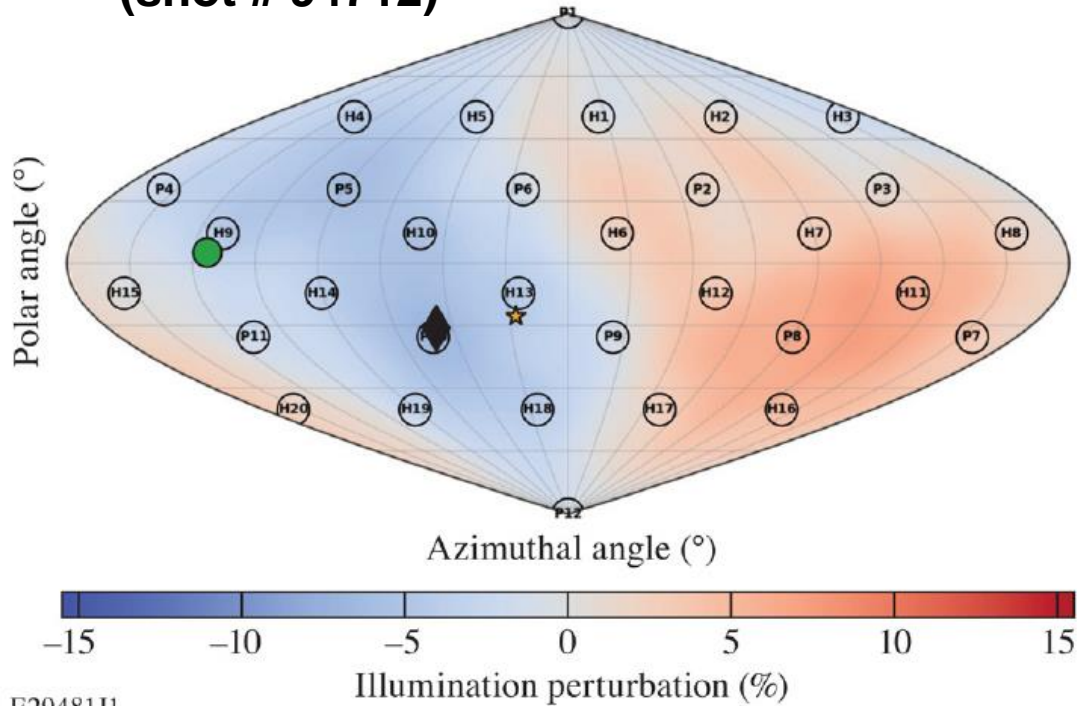
- Higher picket (increases adiabat)
- Shorter pulse
- Increasing average power



Performance improved by increasing adiabat, coupled energy and implosion velocity, and by reducing degradation from He³ with short 3-day DT fills.

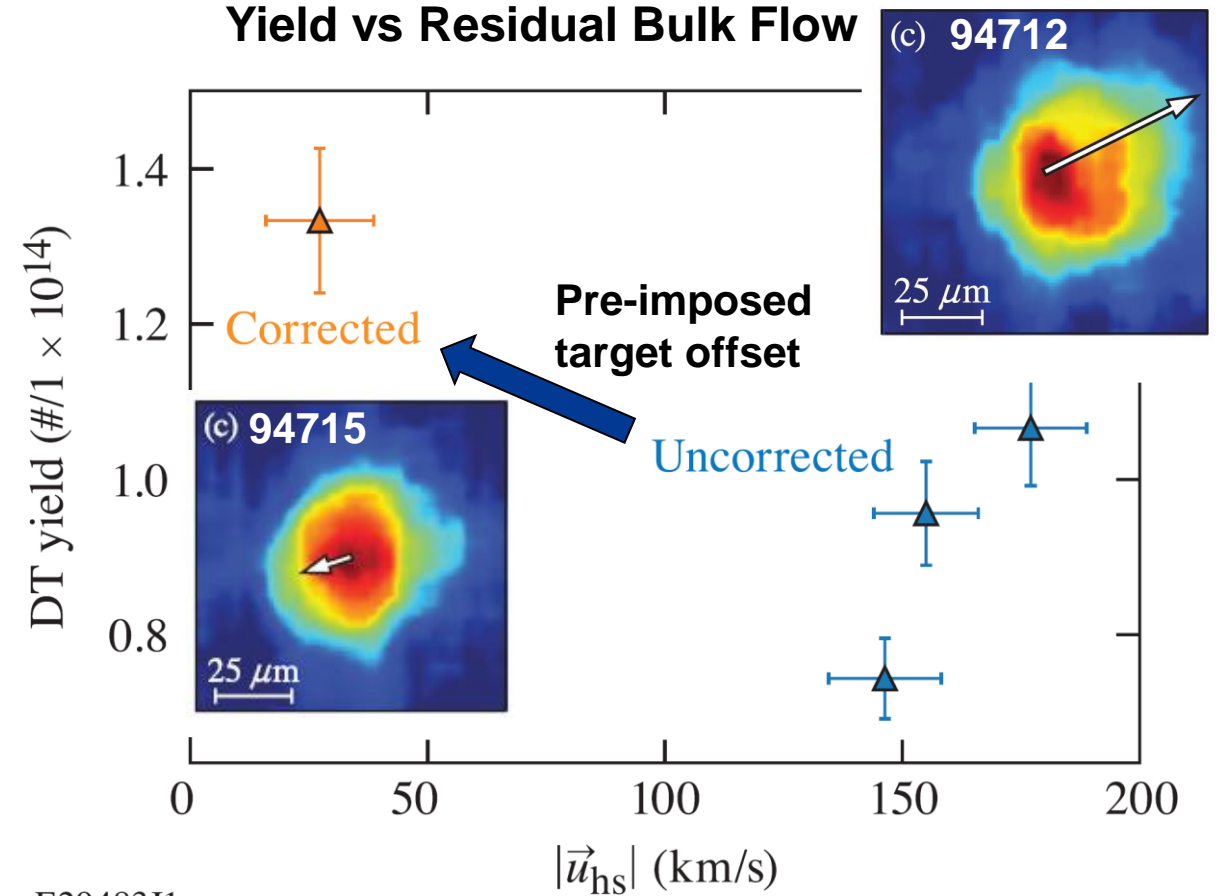
The degradation from mode 1 was mitigated through a pre-imposed offset obtained from nuclear measurement of the residual bulk flow

Hard-sphere projection of laser illumination (shot # 94712)



E29481J1

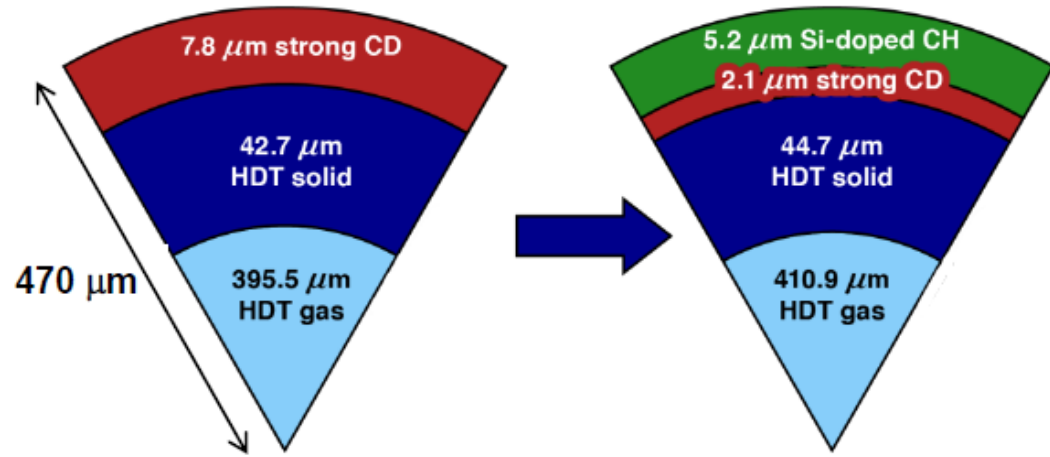
Yield vs Residual Bulk Flow



E29483J1

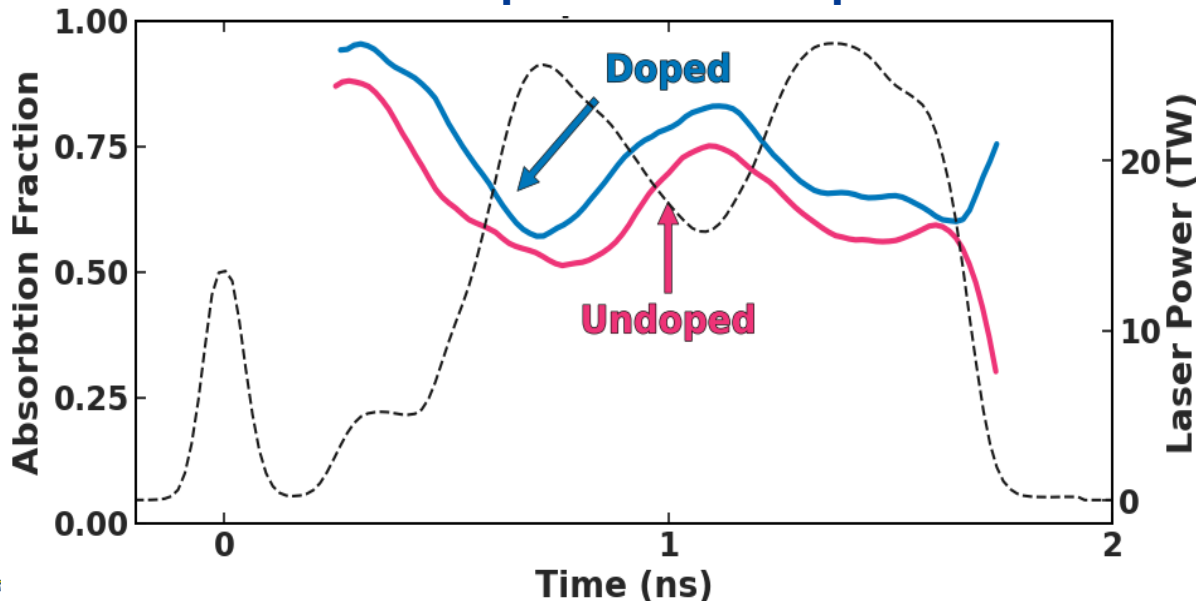
O Mannion et al, Phys. Plasmas 28, 042701 (2021)

Implosion energetics was recently improved by using 6% Si-doping in outer shell to increase laser absorption and suppress laser-plasma instabilities

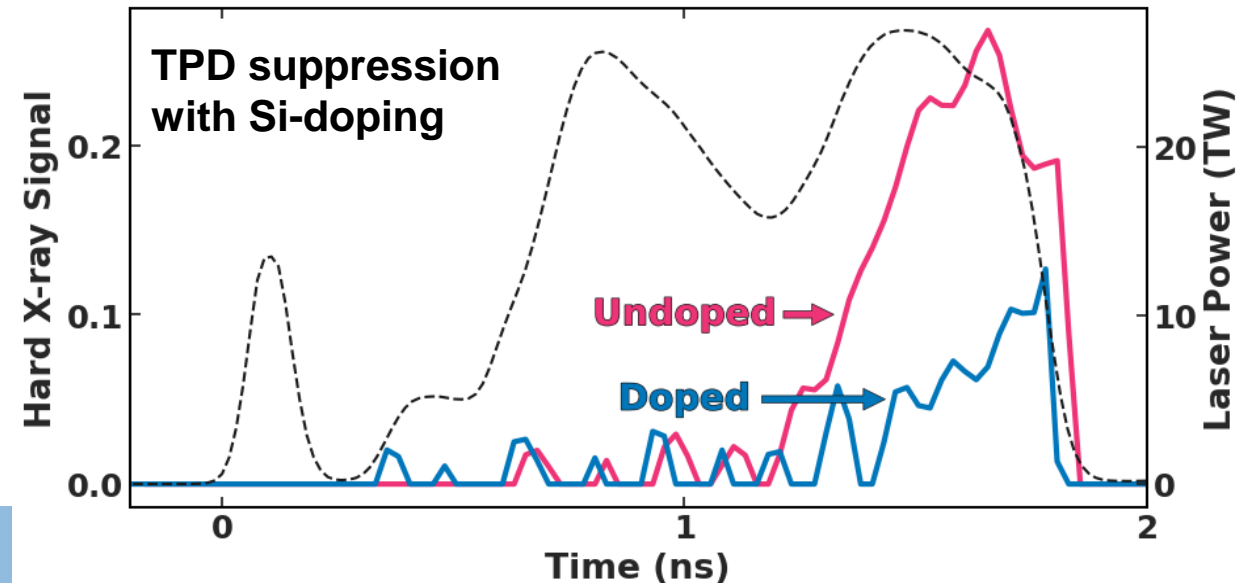


Shot 104949 (best performer, $\alpha_F=5$)
 Laser energy = 28.5 kJ
 Yield = 2.1×10^{14} (0.6 kJ)
 $\rho R = 160 \text{ mg/cm}^2$
 $\chi(2.1 \text{ MJ}) \approx 0.85$

Time dependent absorption

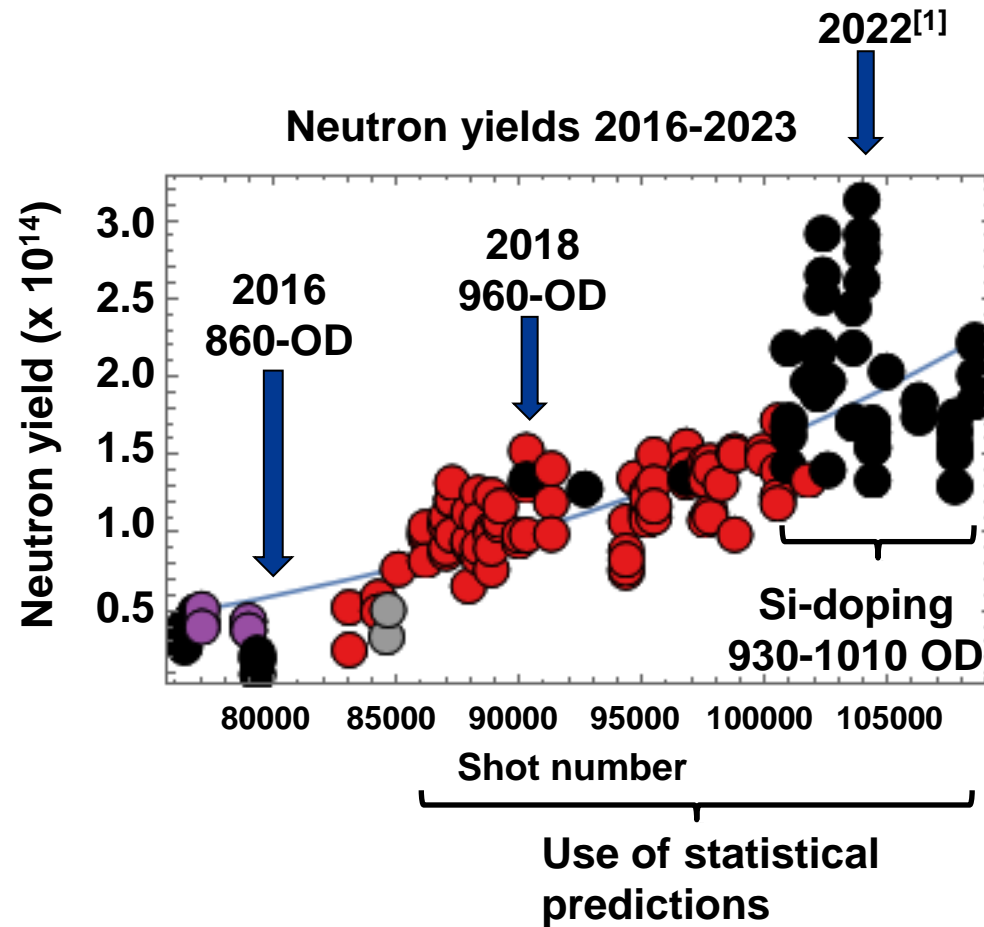


Hard X-ray signal from hot electrons (> 40keV)

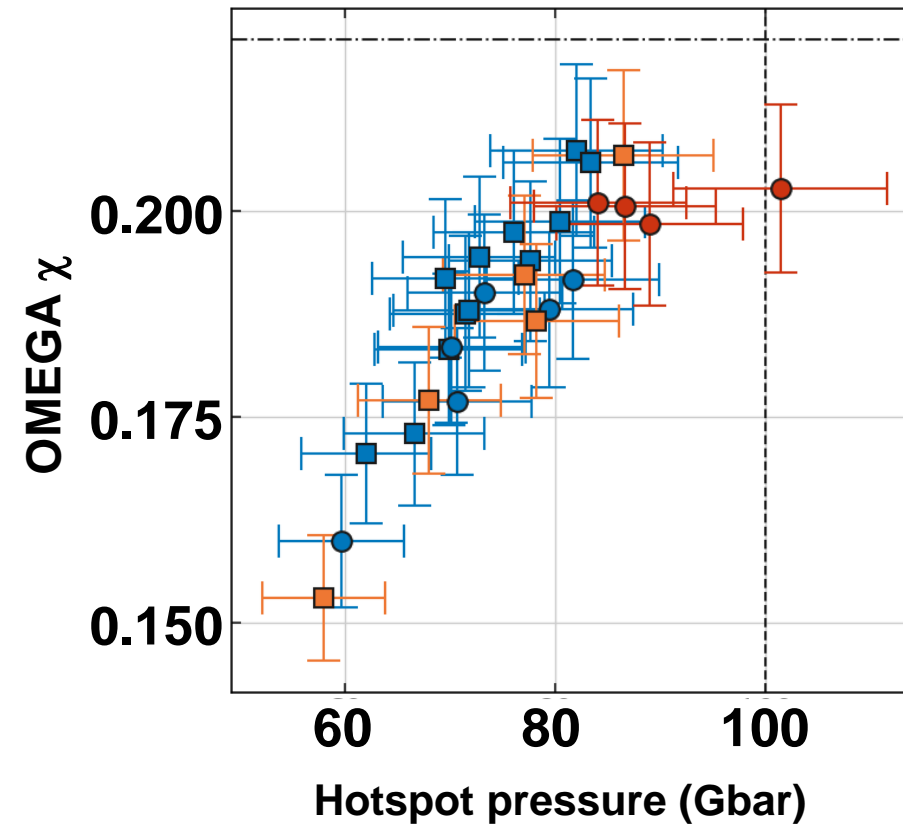


Current performance metrics for OMEGA implosions

Fusion yield, Lawson parameter and hot spot pressure were improved through SM-guided designs and better energy coupling

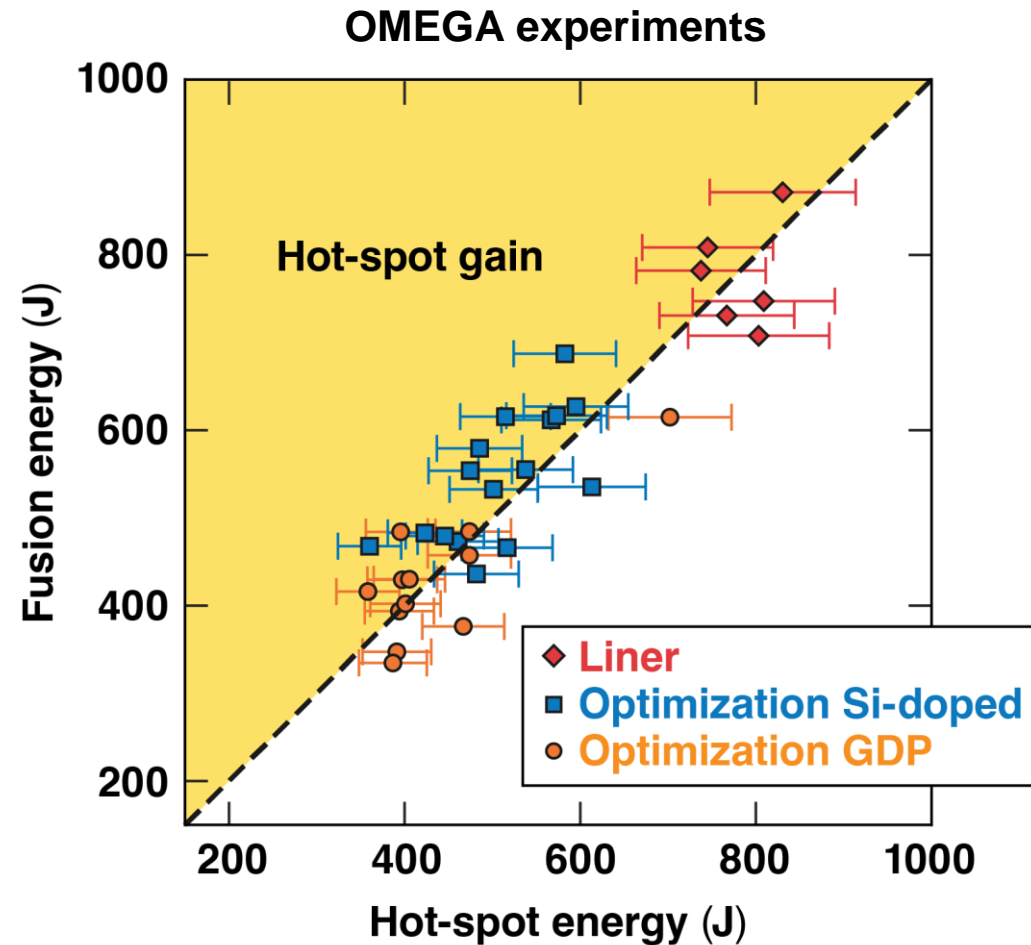


Lawson parameter χ vs hotspot pressure



[1] Record yield achieved with high velocity DT liners
(C. Williams PoP 2021)

Fusion energy outputs exceeding the internal energy of the fusing plasma were achieved on OMEGA (hotspot fuel gain > 1)



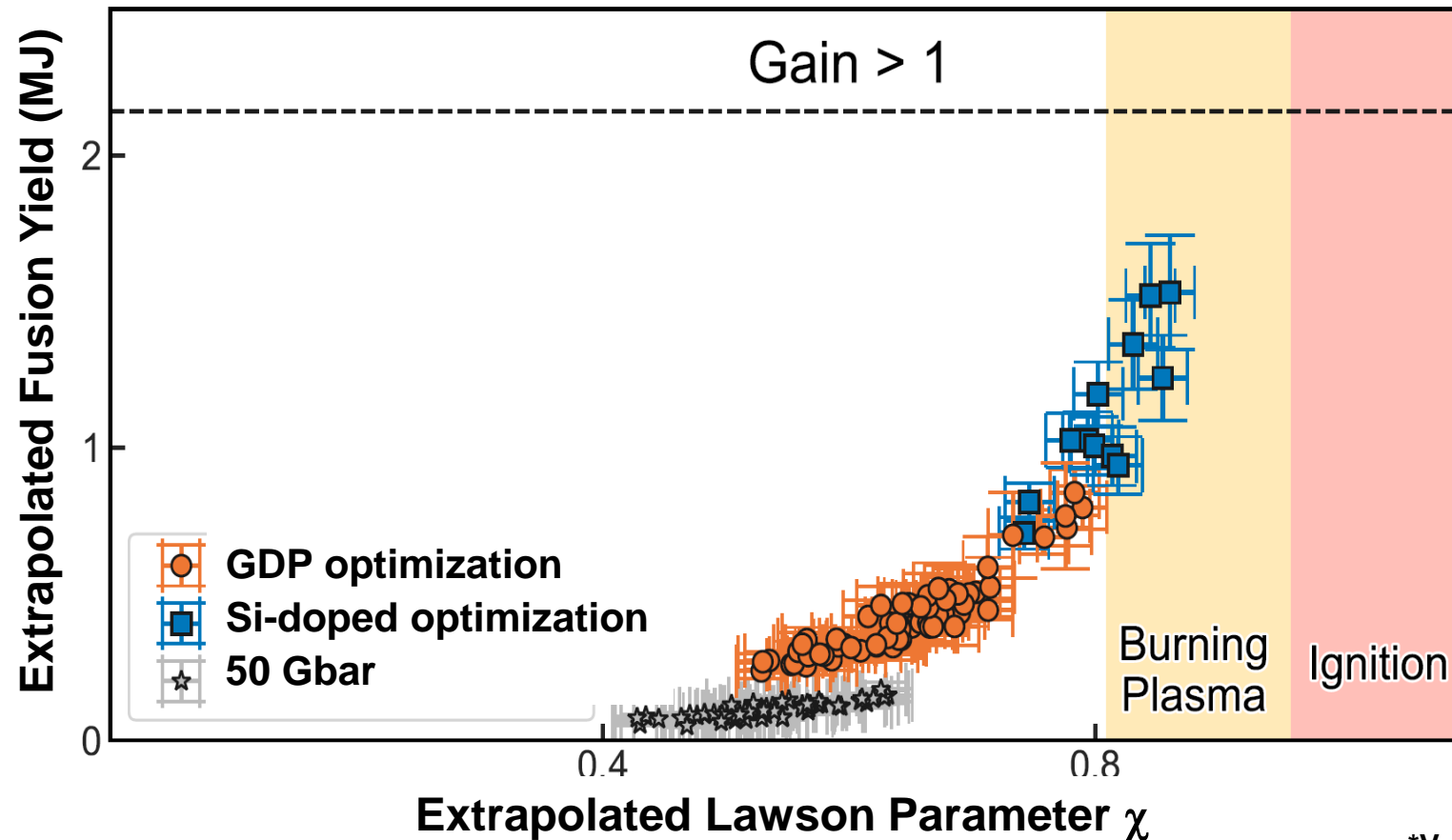
TC16273

$$\text{Gain}_{\text{HS}} = \text{Fusion Energy} / \text{Hot-spot Energy at } R_{17}^{18\text{keV-xray}}$$

C. Williams et al, submitted to Nature Physics

When hydrodynamically extrapolated to 2.1MJ of laser energy, the performance of OMEGA implosions is expected to enter the burning plasma regime

Fusion yield vs χ extrapolated to 2.1 MJ of laser energy*



$$\chi \sim R \sim E_L^{1/3}$$

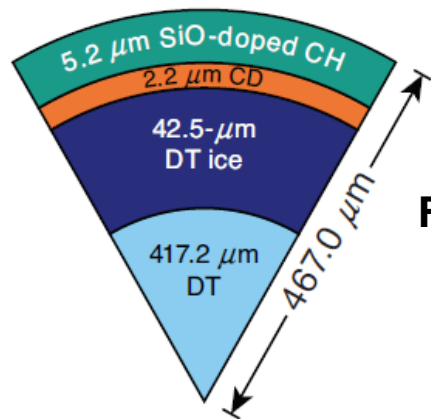
Uses 1D & 2D rad-hydro simulations and analytic models

*V. Gopalswamy et al, submitted to Nature Physics

Upcoming implosion experiments in FY 24

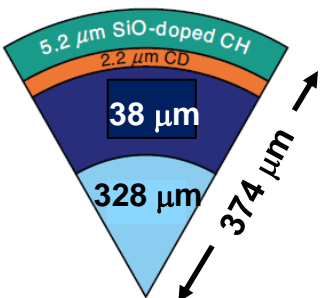
Optimization at smaller scale enables the exploration of a larger parameter space that includes higher intensities and higher ablation pressures

Beam diam 850 μ m

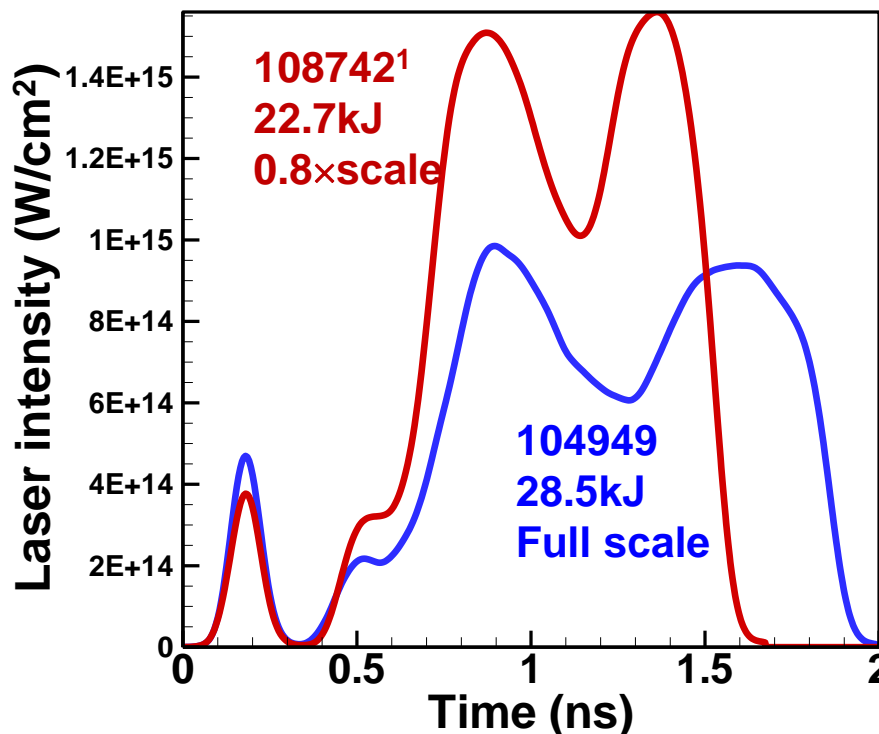


Full scale

Beam diam 650 μ m



0.8 \times scale

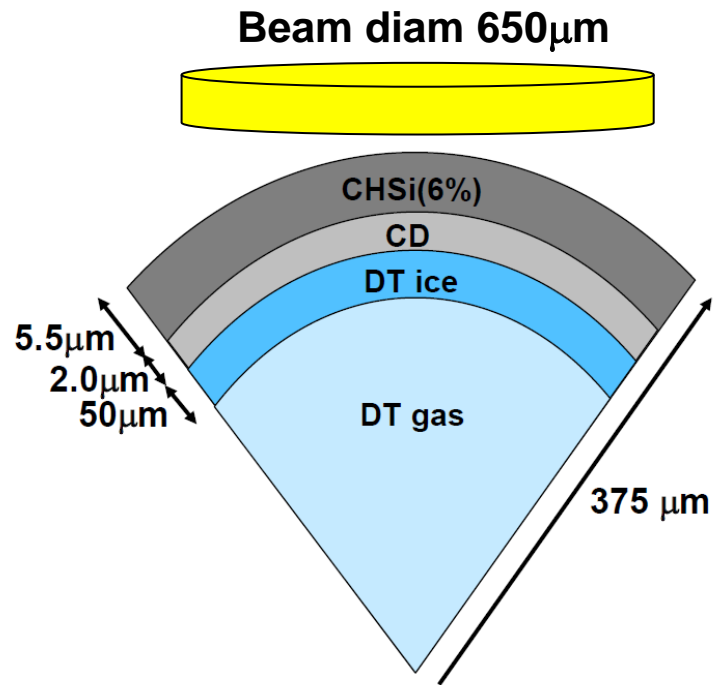


108742¹ - 0.8 \times scale
 $E_{\text{laser}} = 22.7\text{kJ}$
 Yield = 1.4e14
 Fill age = 8 days
 $\chi(2.1\text{MJ})_{\text{adjusted}} = 0.85$

104949 – full scale
 $E_{\text{laser}} = 28.5\text{kJ}$
 Yield = 2.1e14
 Fill age = 3 days
 $\chi(2.1\text{MJ}) = 0.85$

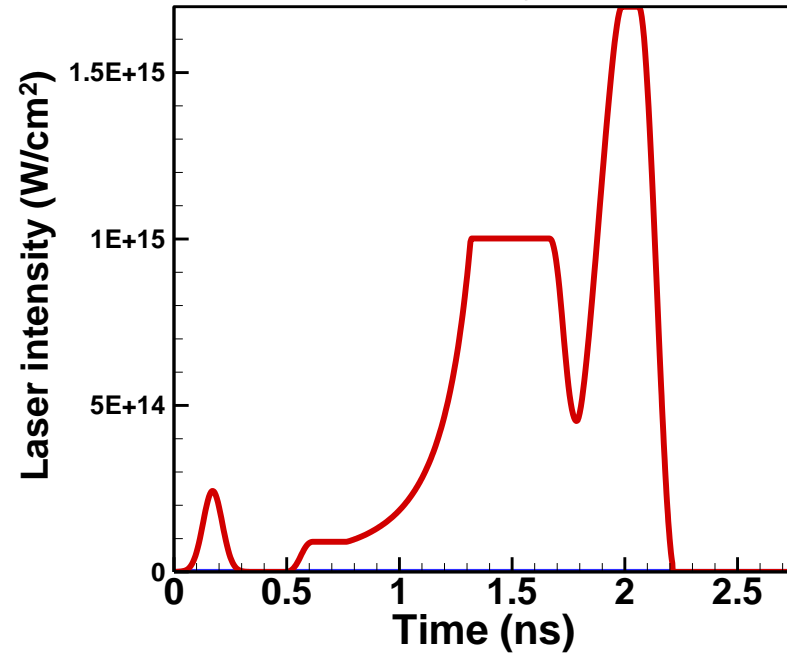
Initial optimization experiments at 0.8 \times scale¹ have reached the same scaled Lawson parameter as the full scale

Shock-augmented¹ ignition designs² will be tested in FY24 using small 650 μm beams to achieve high intensities in the shock-launching power-spike

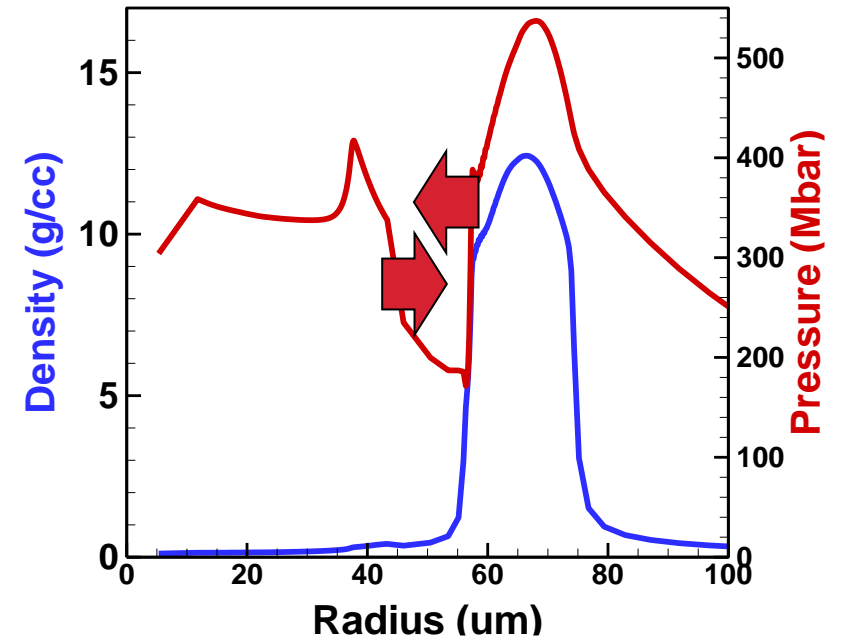


DPP = distributed phase plates

Laser intensity vs Time



Density and pressure at time of shock collision



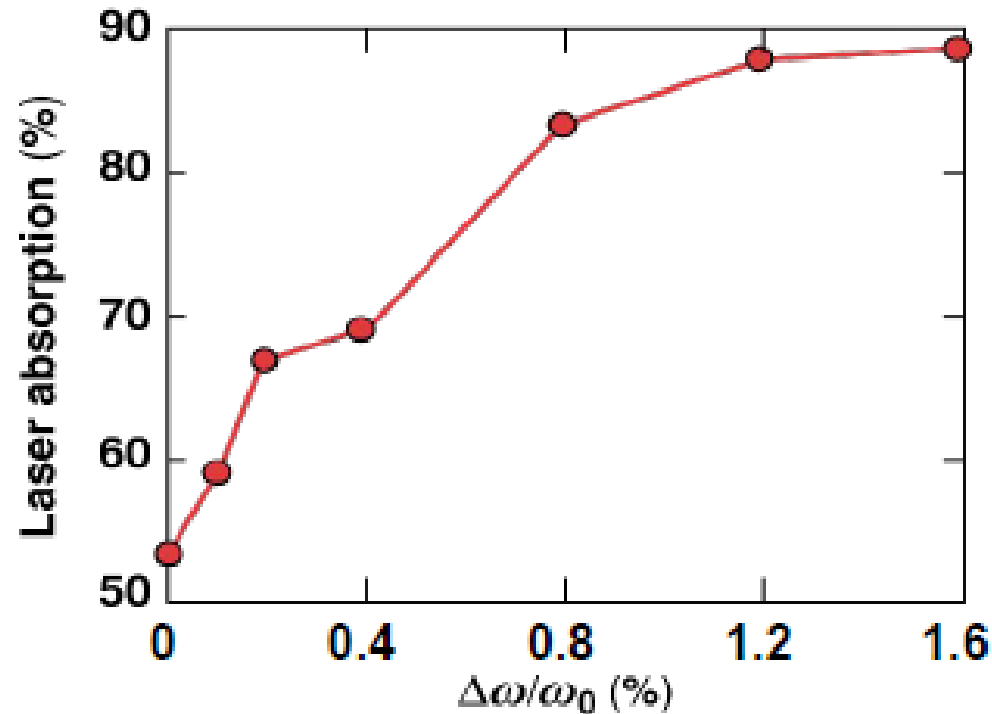
Shock pressures are still well below shock-ignition³ requirements but statistical predictions indicate high values of the extrapolated Lawson parameter

[1] R. Scott et al, Phys. Rev. Lett. 129, 195001 (2021)
[2] Designs by A. Lees (LLE)
[3] R. Betti et al, Phys. Rev. Lett. 98, 155001 (2007)

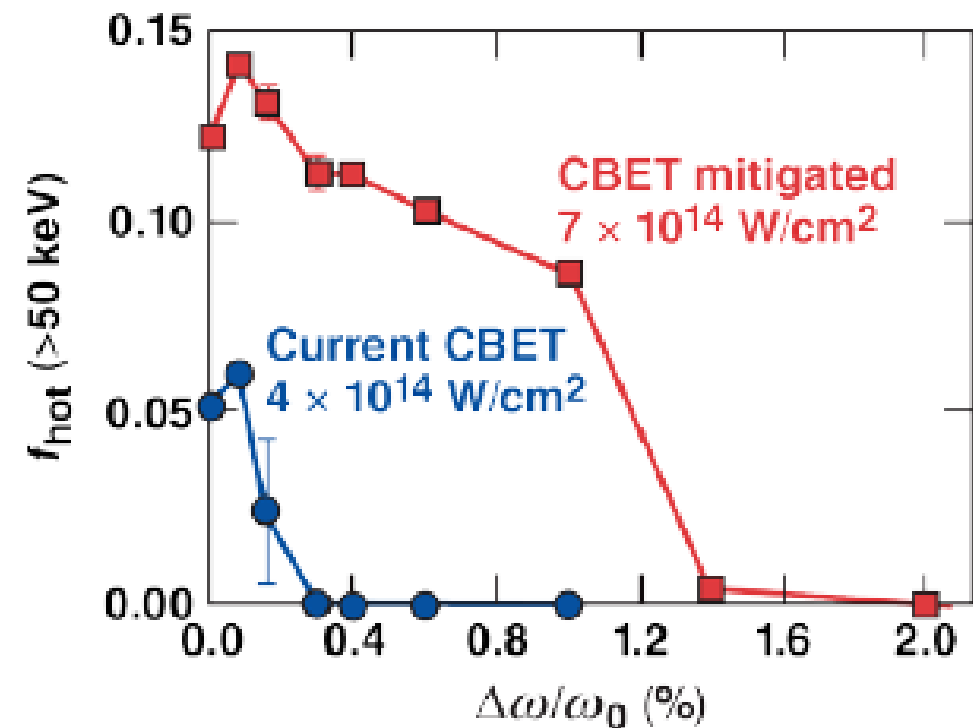
Future improvements: ultrabroadband lasers

Higher performance can be achieved with greater laser bandwidth which improves energetics by suppressing laser-plasma instabilities

Bandwidth suppression of CBET and increase in laser energy absorption¹



Suppression of hot electrons from LPI before and after CBET mitigation²

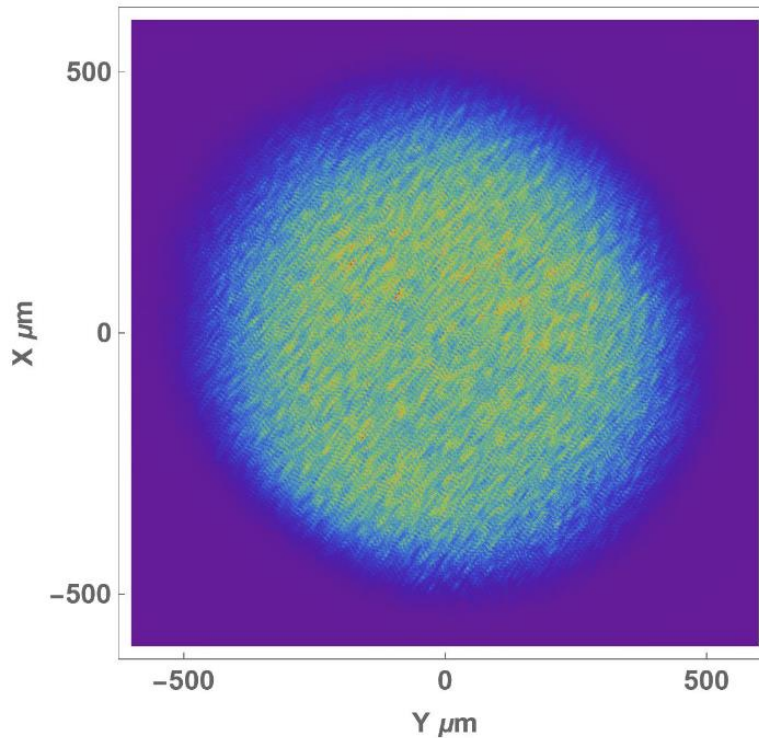


[1] R. Follet et al, Phys. Rev. Lett. 120, 135005 (2018)
[2] R. Follet et al, Phys. Plasmas 28, 032103 (2021)

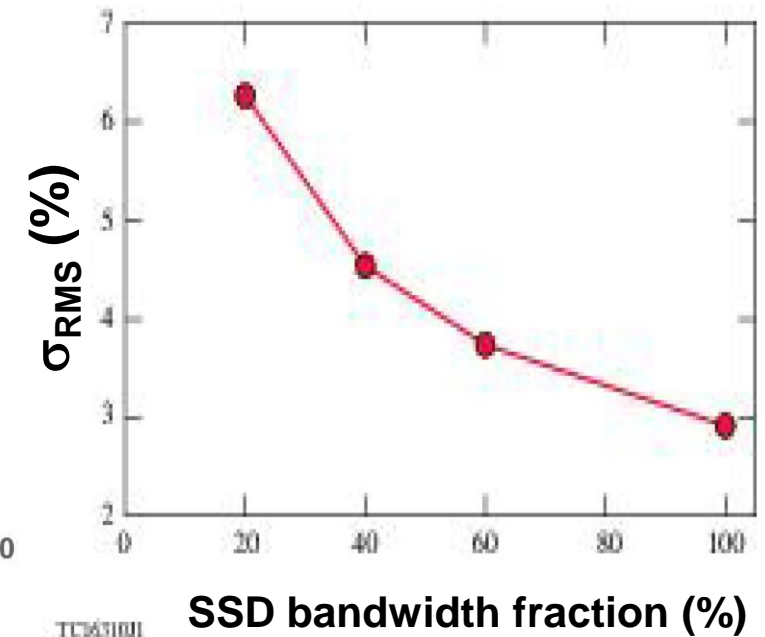
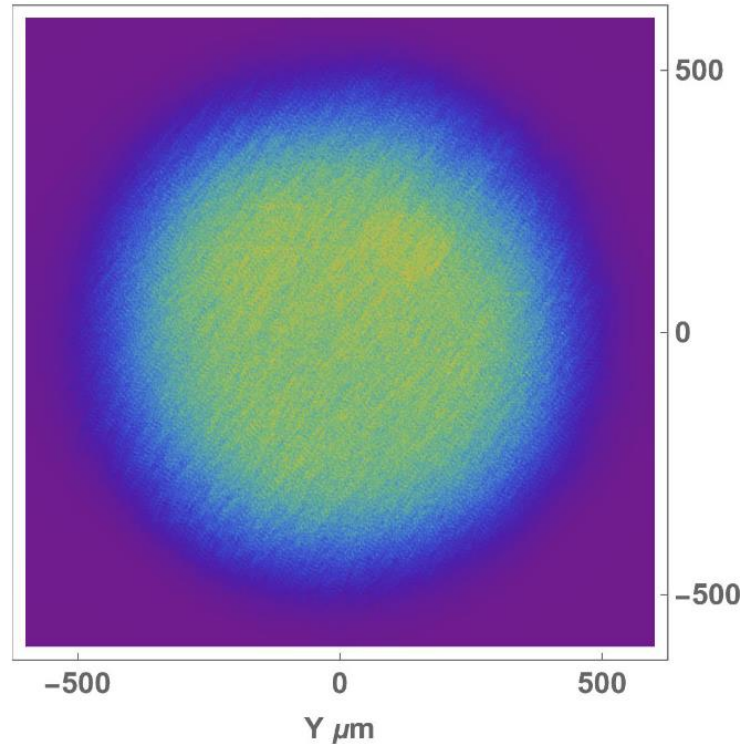
Greater laser bandwidth also reduces speckle amplitude and mitigates laser imprinting

Current OMEGA 300 GHz SSD bandwidth
Measured far-field spatial laser intensity profiles

Beam profile at 20% bandwidth



Beam profile at 100% bandwidth



SSD = smoothing by spectral dispersion

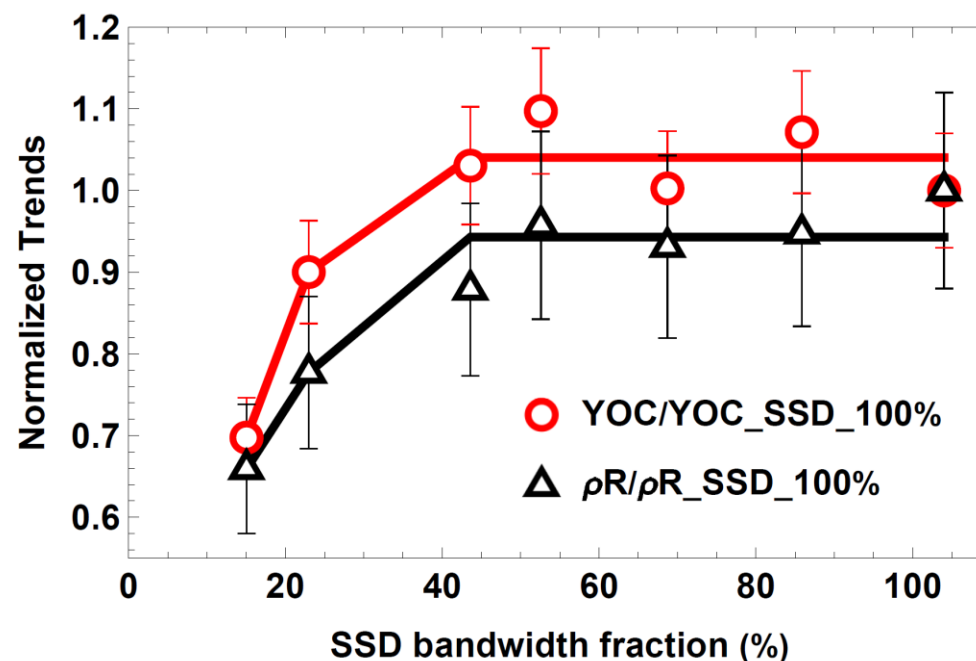
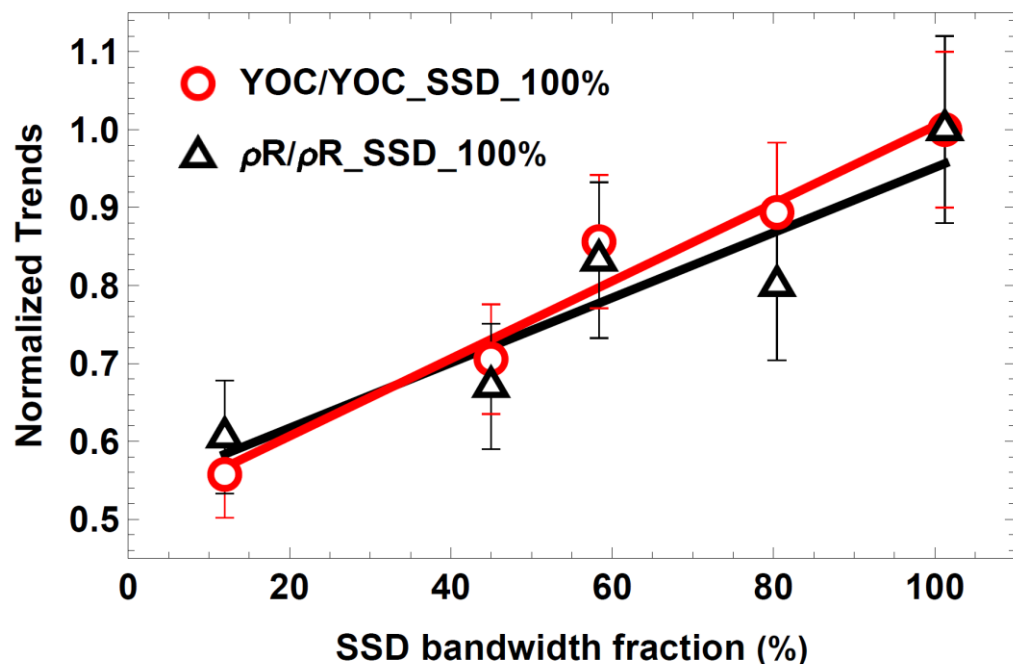
At $\alpha_F=5$, current high performers are insensitive to laser imprinting and SSD bandwidth. Dependency on bandwidth is observed at $\alpha_F=3.5$

SSD = Smoothing by Spectral Dispersion

$$YOC \equiv \frac{\text{Measured Yield}}{\text{Calculated Yield 1D}}$$

$\alpha_F = 3.5$

$\alpha_F = 5$

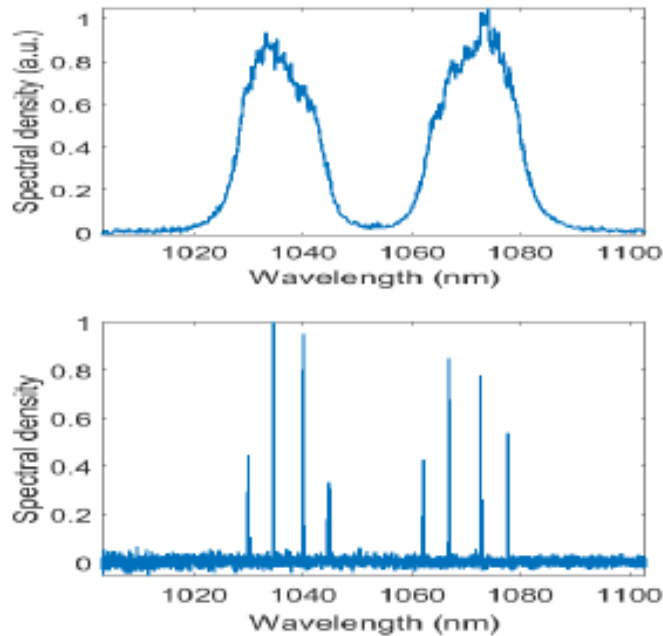


Higher laser bandwidth will enable performing low adiabat implosions

D. Patel, J. Knauer et al, Phys. Rev. Lett. 131, 105101 (2023)

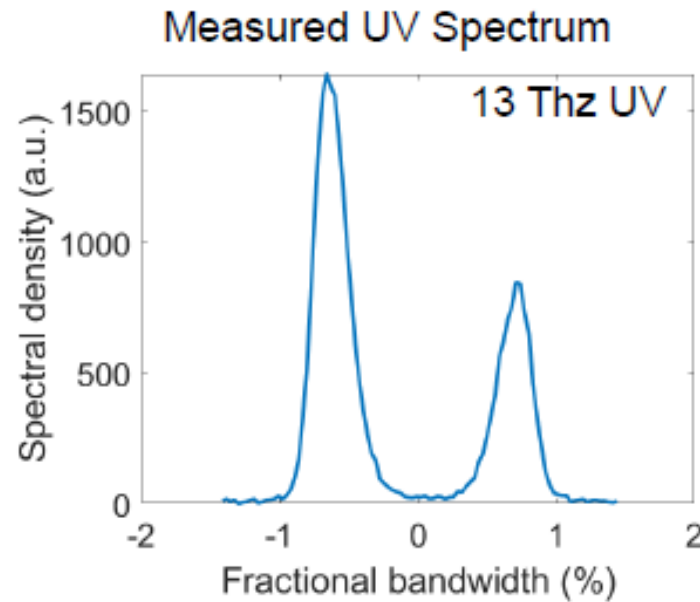
The Fourth generation Laser for Ultrabroadband eXperiments (FLUX) will be commissioned next year and will use the OMEGA LPI platform to validate bandwidth modeling

Ultrabroad Band Laser* (concept demonstration)



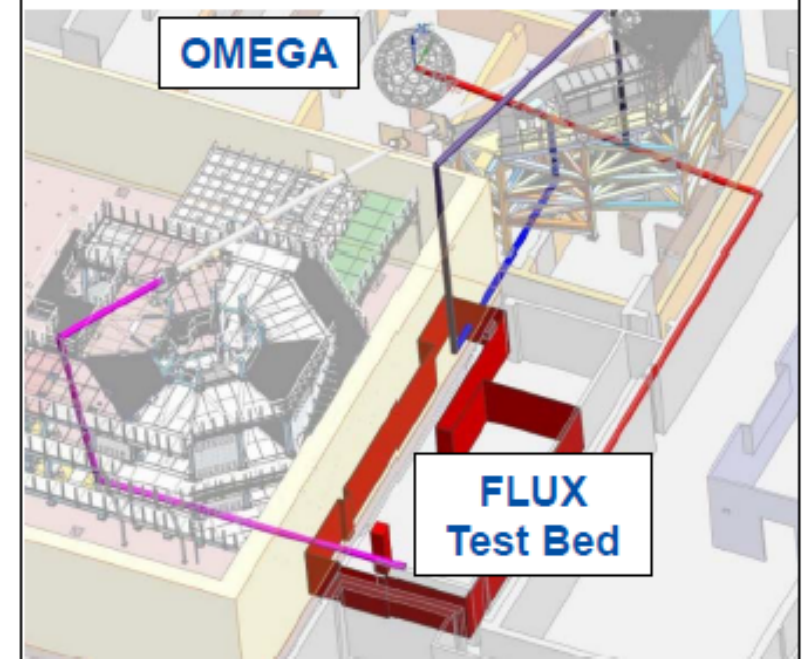
A colinear OPA was used to amplify broad bandwidth long-pulse laser beam

Demonstrated Broadband UV Frequency Conversion**



Novel concept demonstrates efficient broad band ($\Delta\omega/\omega > 1.5\%$) UV frequency tripling

The FLUX laser will feed the OMEGA LPI Platform



FLUX experiments will validate LPI modeling with bandwidth

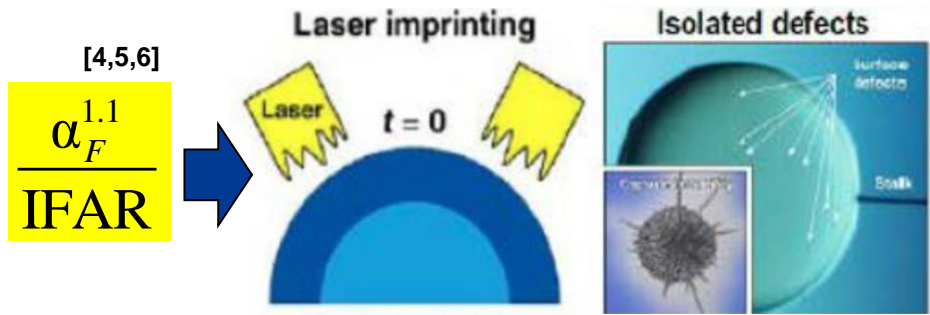
Implosion experiments on OMEGA have achieved record Lawson parameters for direct drive and core conditions that scale to a burning plasma at NIF energies.

- **Data-driven predictive models have been used to design high performance implosions on OMEGA**
- **The Lawson parameter has been improved by increasing coupled energy with larger, Si-doped targets and thinner ice layers**
- **When hydrodynamically extrapolated to 2.1 MJ of symmetric illumination, the best performing OMEGA implosions are expected to be in the burning plasma regime with a fusion yield of about 1.5 MJ**
- **Next generation broadband lasers are expected to improve energy coupling by mitigating laser plasma instabilities and reducing the seeds for hydrodynamic instabilities**

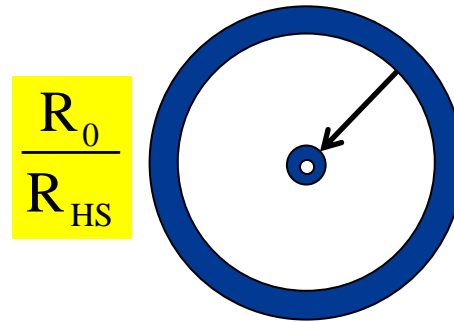
BACK UP SLIDES

Relevant dimensionless parameters are identified¹⁻³ that determine performance degradation in OMEGA implosions

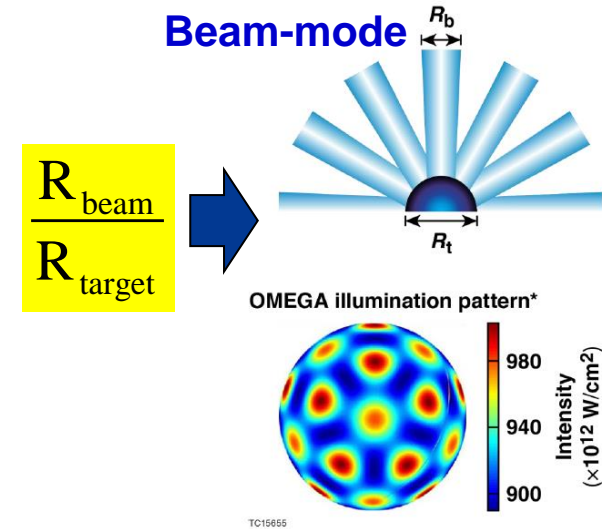
Short wavelength Rayleigh-Taylor (RT)



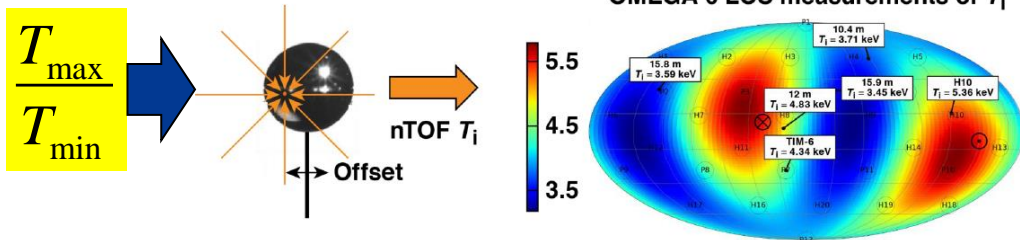
Convergence Ratio



Beam-mode

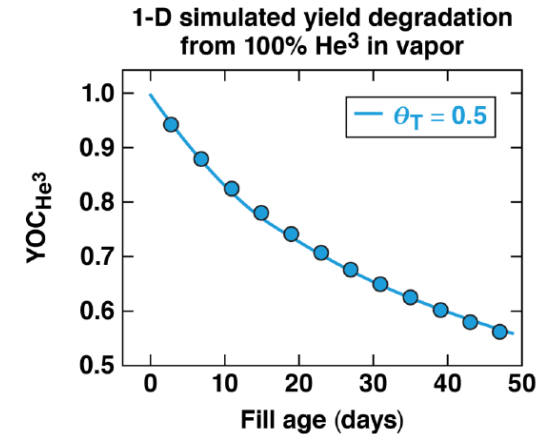


Mode L=1



He³ contamination from tritium decay

$$\text{YOC}_{\text{He}^3}^{\text{sim}(1\text{D})}$$



[1] A. Lees et al, submitted to PoP (2022)
[2] A. Lees et al, Phys. Rev. Lett. 127, 105001 (2021)

[3] V. Gopalswamy et al, Phys. Plasmas 28, 122705 (2021)
[4] V. Goncharov et al, Phys. Plasmas 21, 056315 (2014)

[5] H. Zhang et al, Phys. Rev. Lett.
[6] H. Zhang et al, Phys. Plasmas 27, 122701 (2020)

A major goal for LLE is to produce scaled ignition conditions on OMEGA for direct drive. Hydrodynamic scaling is used to extrapolate OMEGA implosion performance to larger laser energies typical of the NIF

The measurable normalized ignition condition is determined by the Lawson parameter for ICF¹⁻⁴

$$\chi_{\text{exp}} = \frac{nT\tau}{[nT\tau]_{\text{ign}}} \sim \left[(\rho R)^2 \left(\frac{Y_{DT}}{M_{DT}} \right) \right]^{1/3}$$

The Lawson parameter increases linearly with scale, giving the condition for scaled ignition

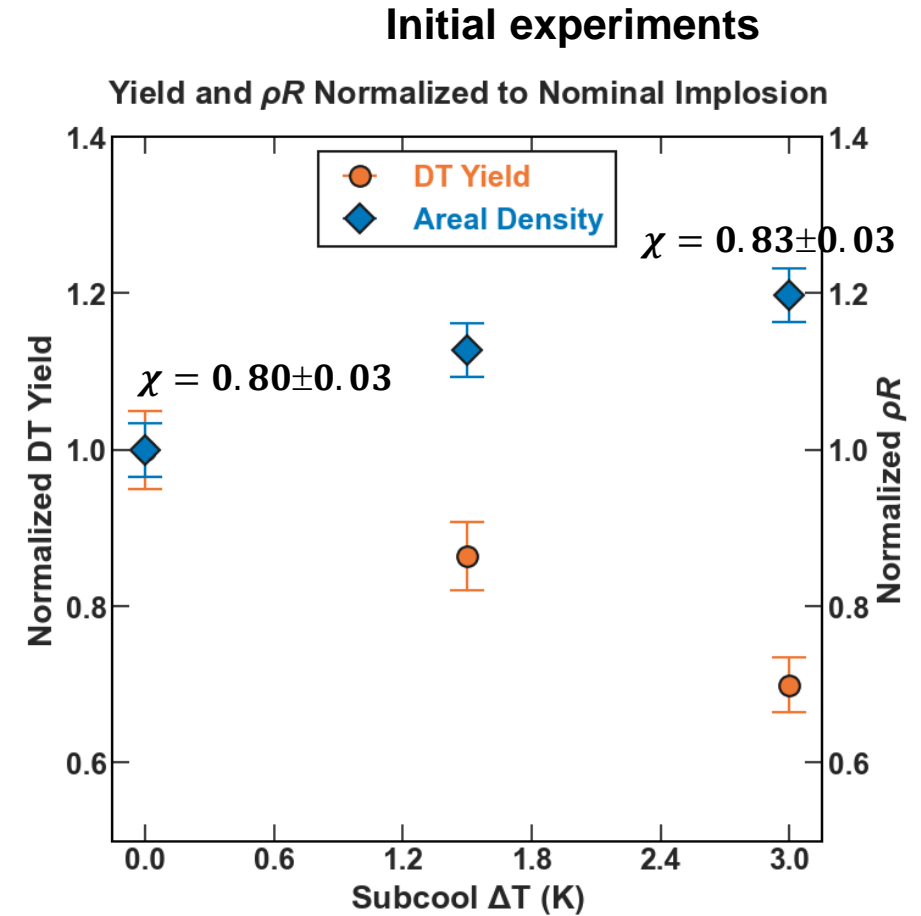
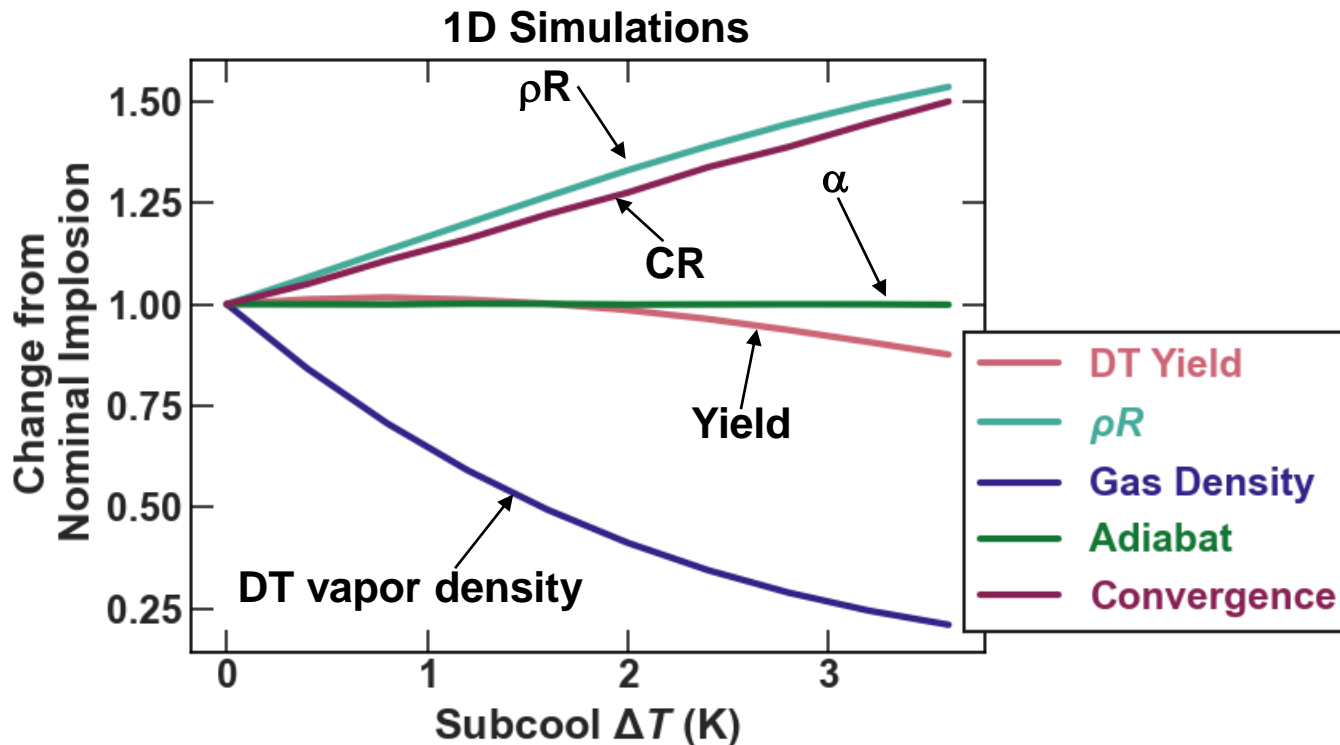
$$\chi_{\text{scaled}} \sim \tau \sim R \sim E_{\text{Laser}}^{1/3} \quad \longrightarrow \quad \chi_{\text{scaled}} \equiv \chi_{\text{OMEGA}} \left(\frac{E_L^{\text{scaled}}}{E_L^{\text{OMEGA}}} \right)^{1/3} > 1$$

Hydroequivalent Ignition is $\chi = 1$ at NIF energies of 2.1 MJ

Initial experiments show that ρR and CR increase with subcooling while the fusion yield decreases. Overall impact points to higher Lawson parameter



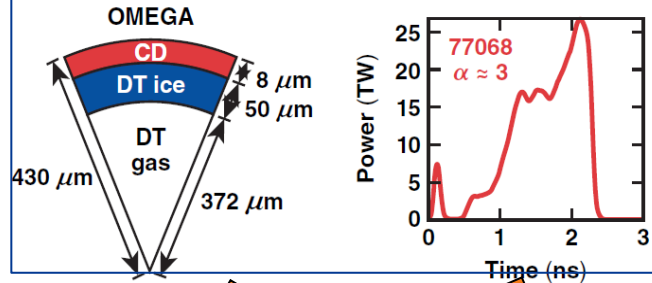
Subcooling below the triple point leads to higher convergence without changes to the adiabat



Experiments by J. Knauer, L. Ceurvorst and V. Gopalswamy

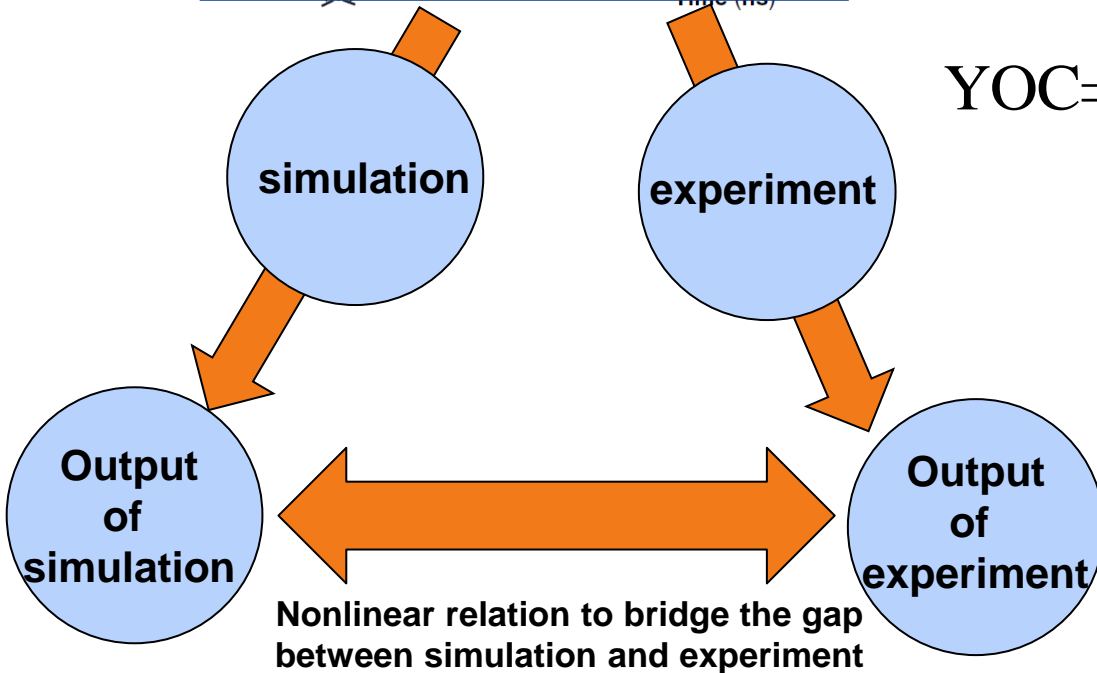
Statistical mapping or DNN can be used to bridge the gap between simulations and experiments to develop a predictive capability and understand degradation sources

Laser pulse and target specifications are inputs to both the code and the experiment



$$\text{YOC} = \text{Yield Over Clean} = \frac{\text{Yield measured}}{\text{Yield 1D simulation}}$$

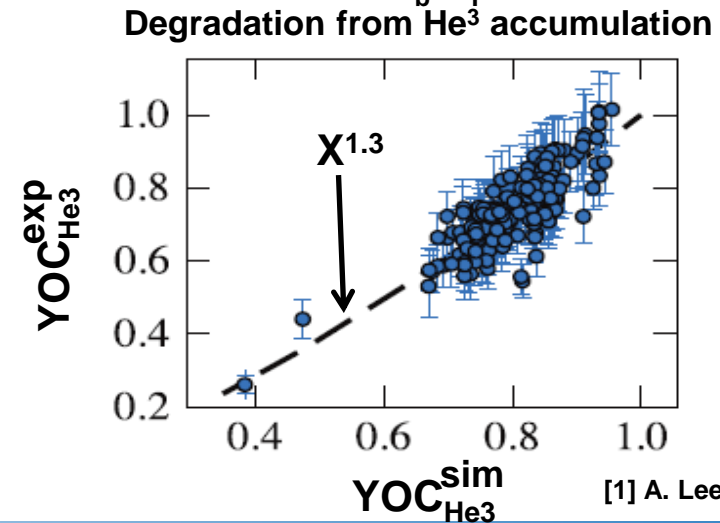
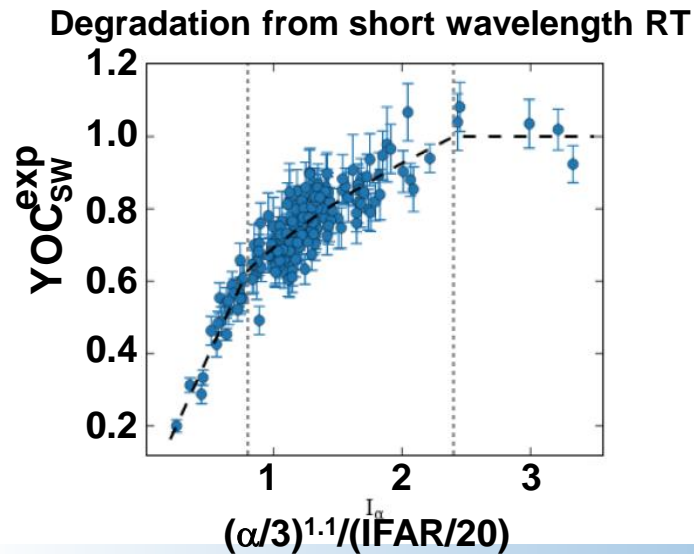
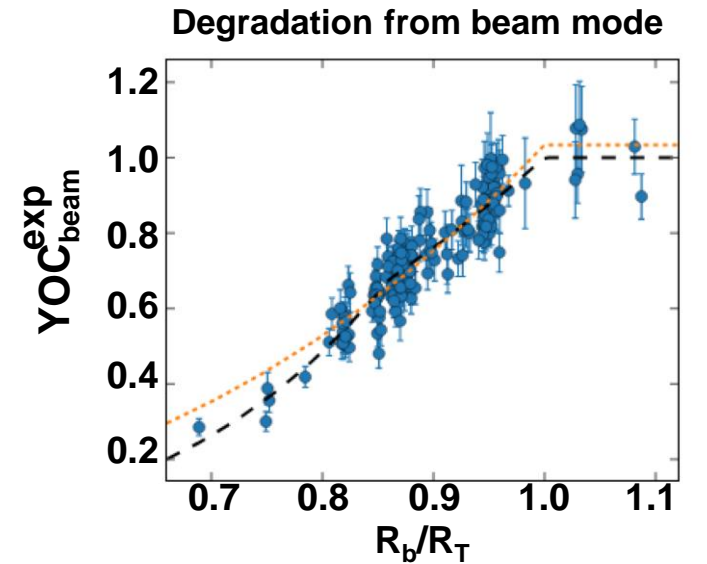
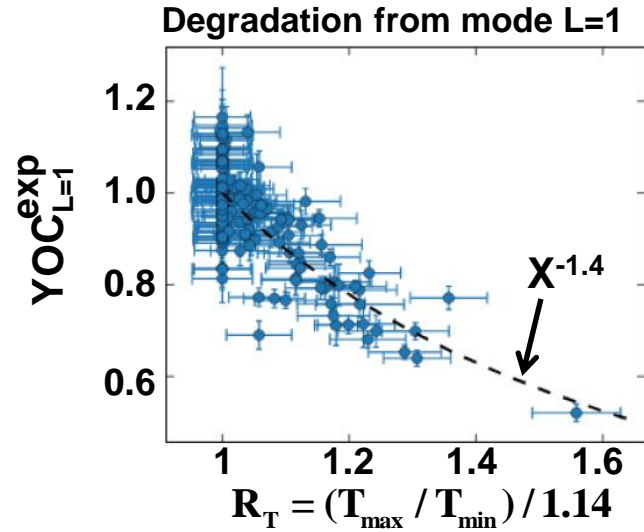
$$\text{YOC} = \text{YOC}_{\text{stab}}(\alpha, \text{IFAR}, \text{CR}) \text{YOC}_{\text{beam}} \left(\frac{R_b}{R_t} \right) \text{YOC}_{L=1} \left(\frac{T_{\text{max}}}{T_{\text{min}}} \right) \dots$$



[1] V. Gopalswamy et al, Nature 565, 581-586 (2019)

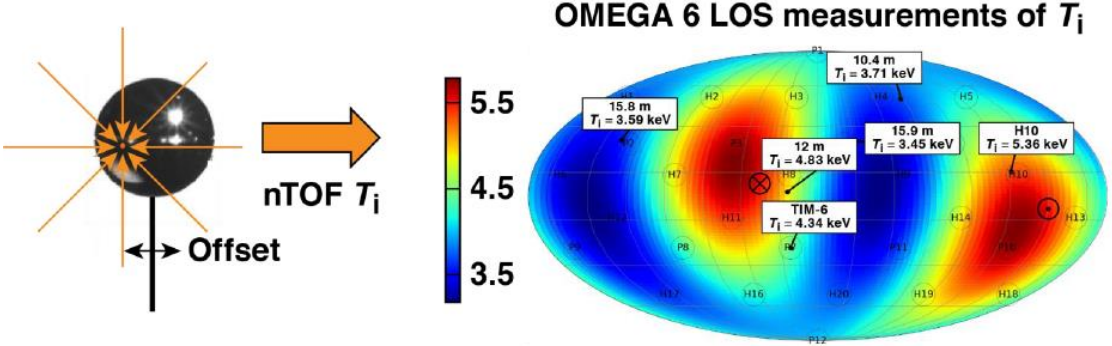
[2] A. Lees et al, Phys. Rev. Lett. 127, 105001 (2021)

Each degradation mechanism can be isolated and quantified¹

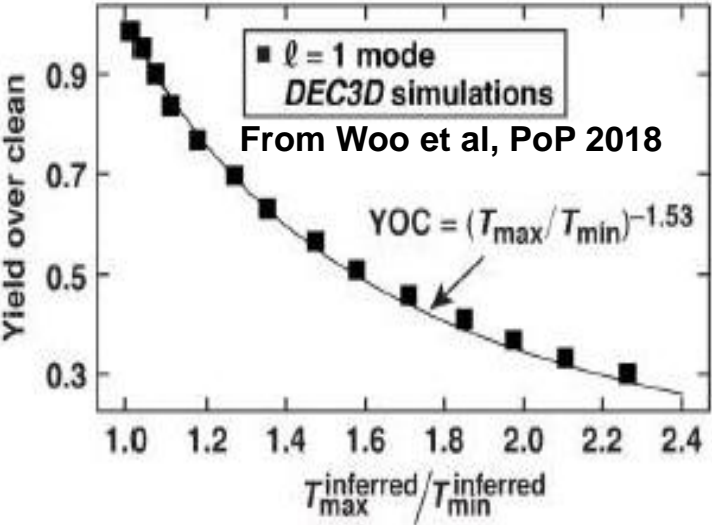


[1] A. Lees et al, Phys. Rev. Lett. 127, 105001 (2021)

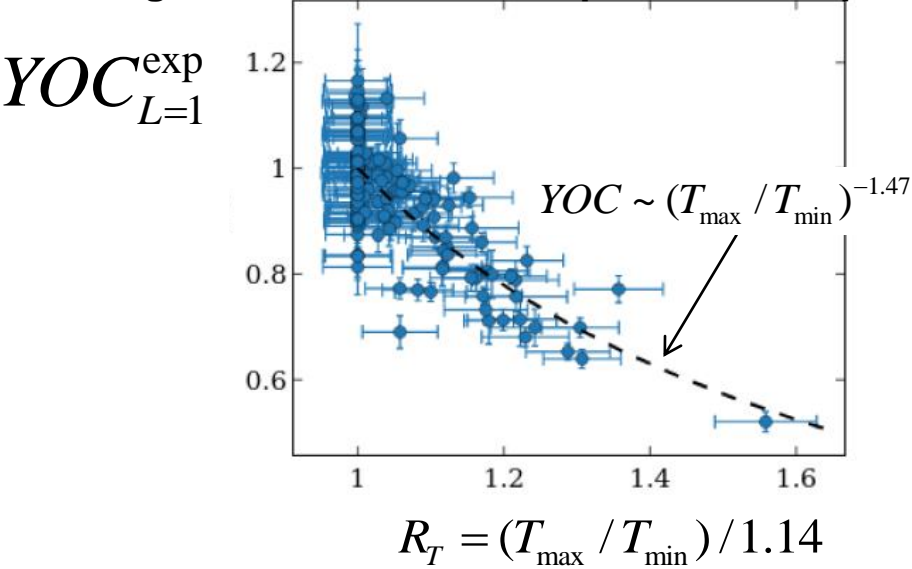
The effects of mode L=1 from offset and mispointing are assessed through the measured T_i asymmetries



Degradation from L=1: Simulated dependence

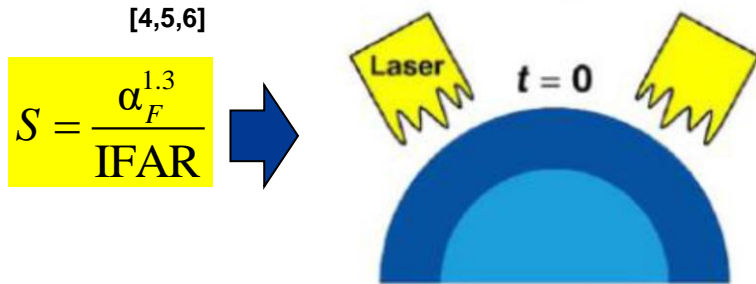


Degradation from L=1: Experimental dependence

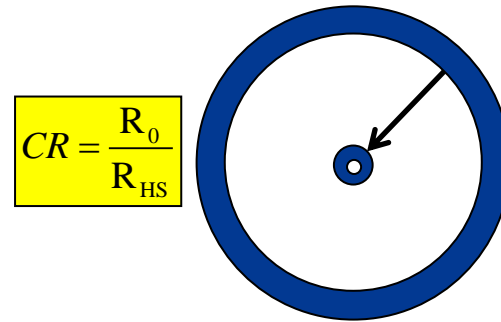


The SM uses mapping of experimental data onto simulated dimensionless parameters¹⁻³ determining performance degradation

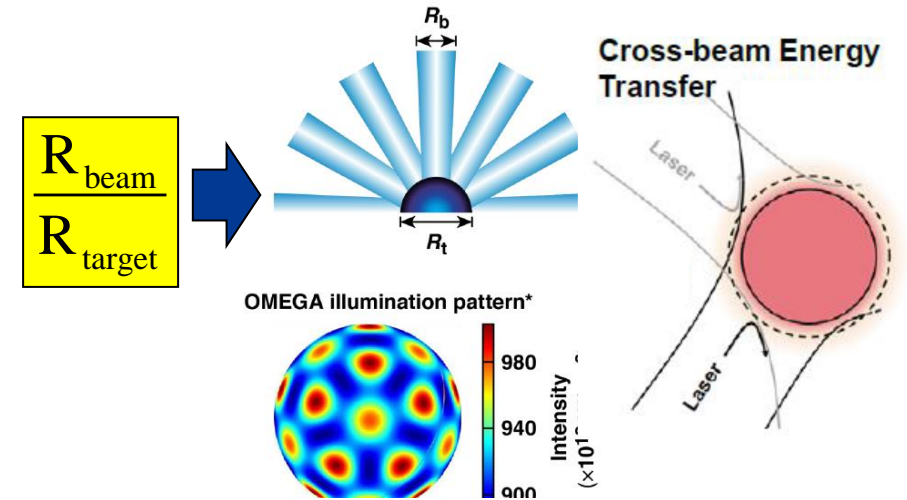
Short wavelength Rayleigh-Taylor (RT)



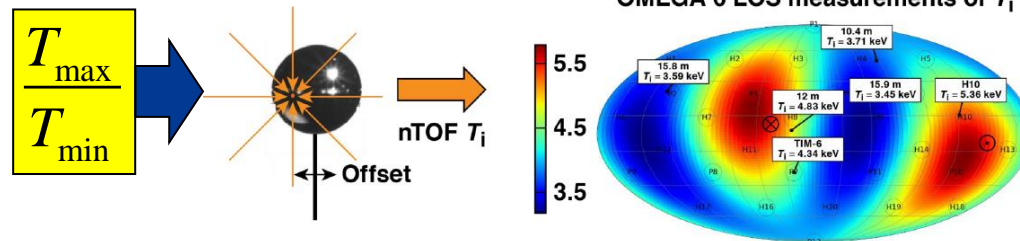
Convergence Ratio



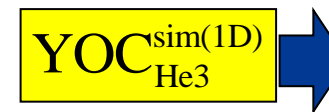
Beam-mode and CBET



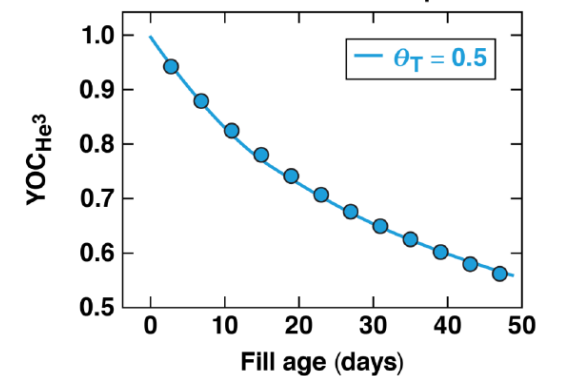
Mode L=1



He³ contamination from tritium decay



1-D simulated yield degradation from 100% He³ in vapor



[1] A. Lees et al, submitted to PoP (2022)

[2] A. Lees et al, Phys. Rev. Lett. 127, 105001 (2021)

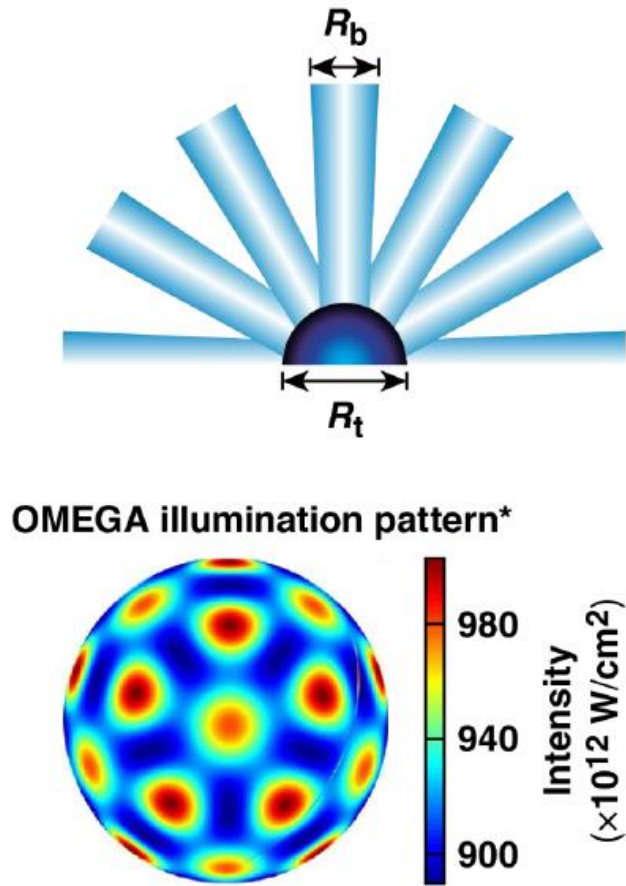
[3] V. Gopalswamy et al, Phys. Plasmas 28, 122705 (2021)

[4] V. Goncharov et al, Phys. Plasmas 21, 056315 (2014)

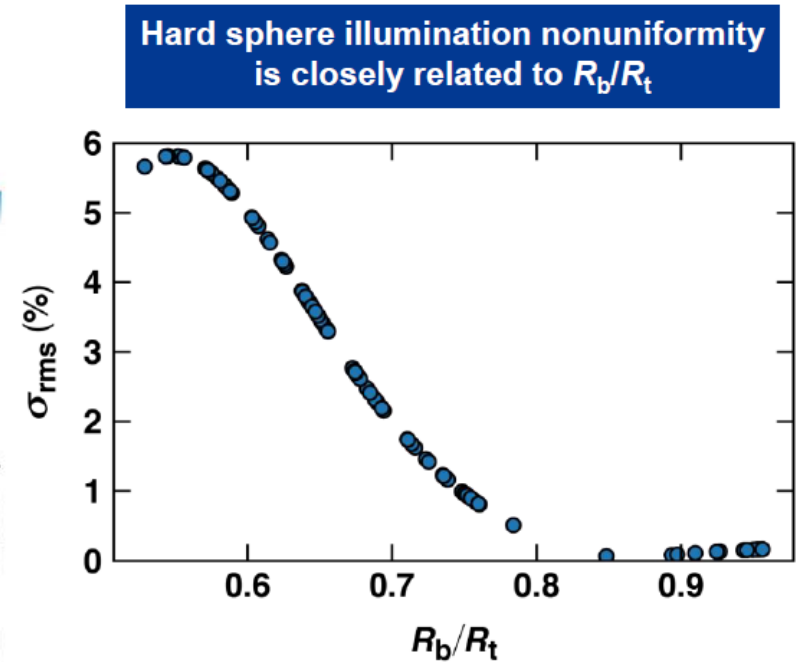
[5] H. Zhang et al, Phys. Rev. Lett. (2018)

[6] H. Zhang et al, Phys. Plasmas 27, 122701 (2020)

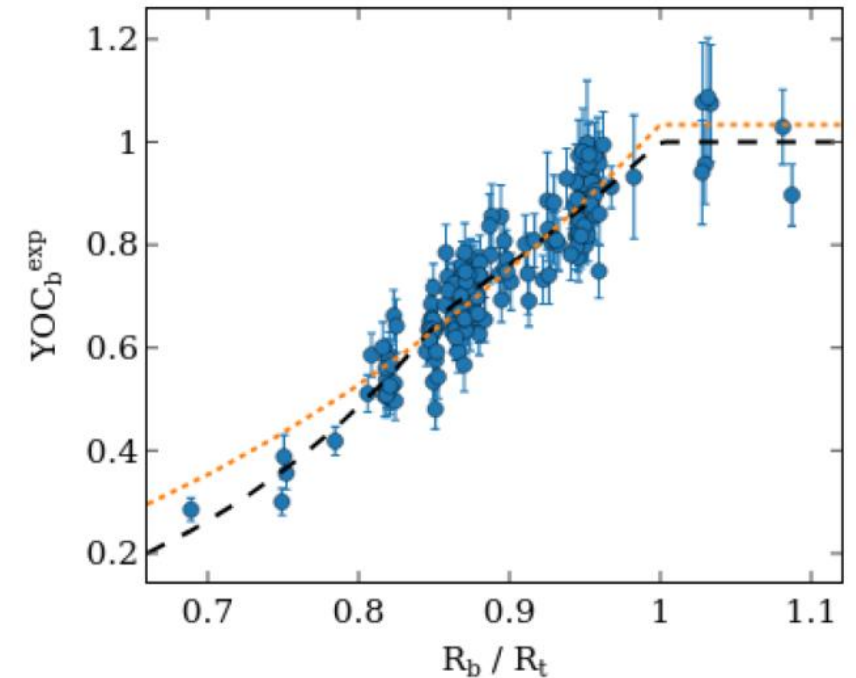
The fusion yield is reduced by the ratio of the laser beam to target radius indicating degradation from laser illumination nonuniformities from port geometry



TC15655



Degradation from beam mode: experimental dependence



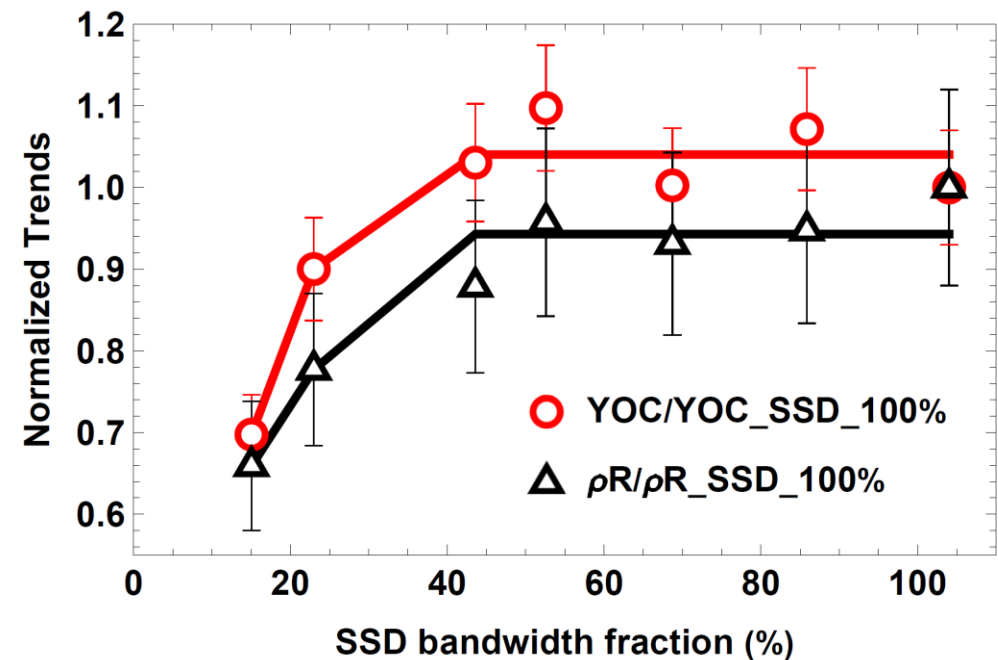
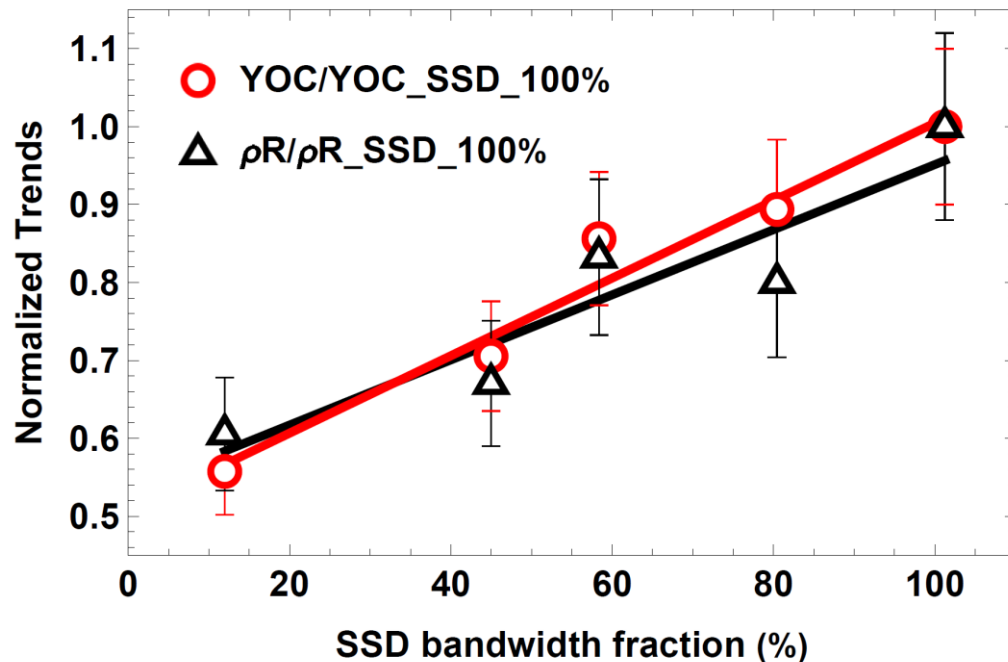
See also A. Colaitis et al, PRL 2022

Laser bandwidth is a dominant lever for mitigating imprinting in low α_F targets. At $\alpha_F=5$, current high performers are insensitive to bandwidth

$$YOC \equiv \frac{\text{Measured Yield}}{\text{Calculated Yield 1D}}$$

$\alpha = 3.5$

$\alpha = 5$

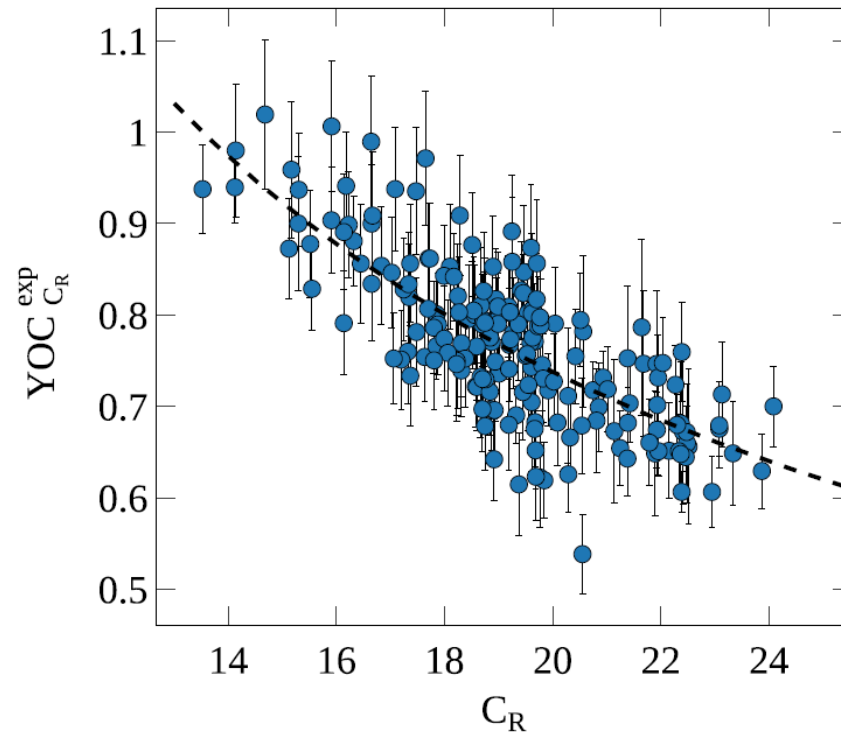


D. Patel, in press in PRL

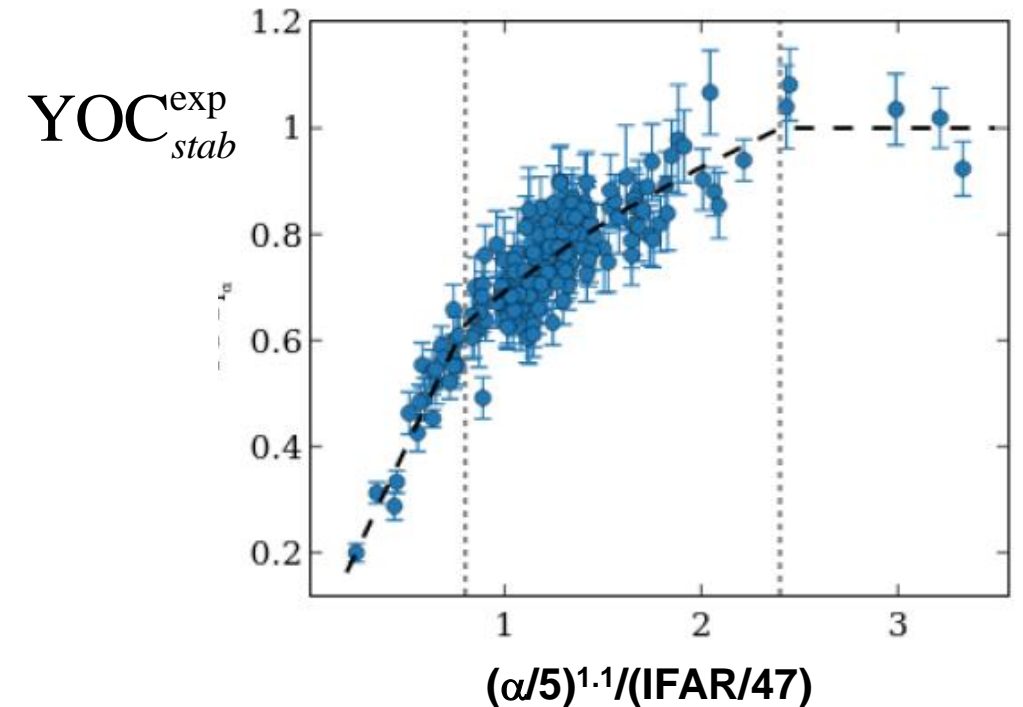
Higher laser bandwidth will enable performing low adiabat implosions

The fusion yield is reduced by short-wavelength Rayleigh-Taylor (probably seeded by laser imprinting) and low and/or mid modes from the laser

Degradation from low or mid modes



Degradation from short wavelength hydro instabilities: experimental dependence



* V. N. Goncharov *et al.*, *Phys. Plasmas* **21**, 056315 (2014).

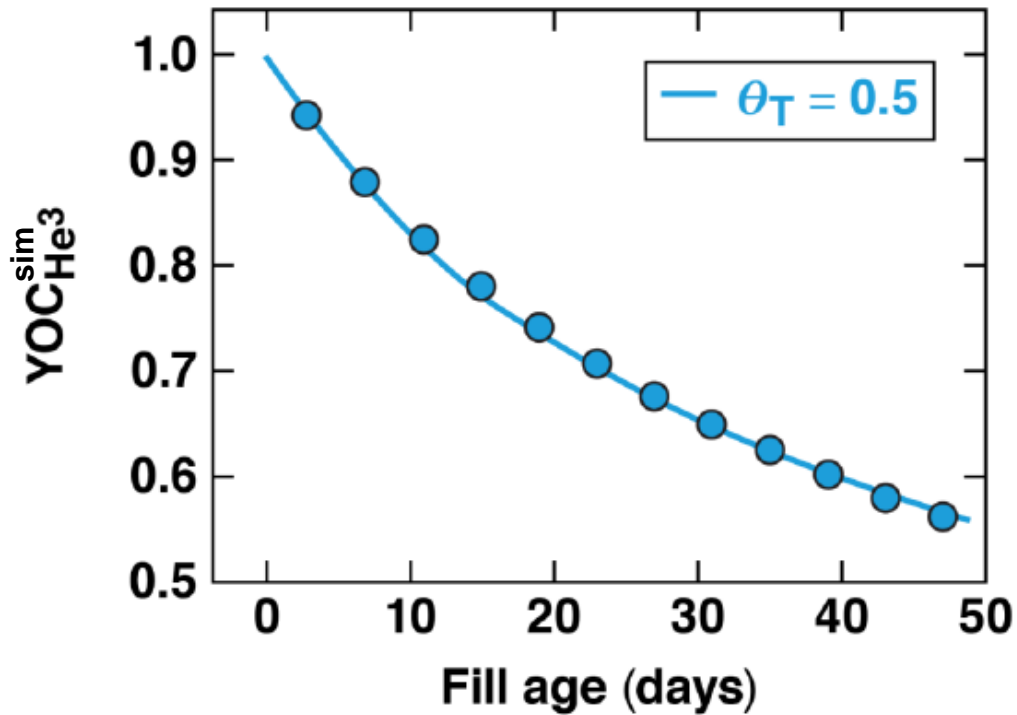
H. Zhang *et al.*, *Phys. Plasmas* **27**, 122701 (2020).

RT: Rayleigh–Taylor

IFAR: in-flight aspect ratio

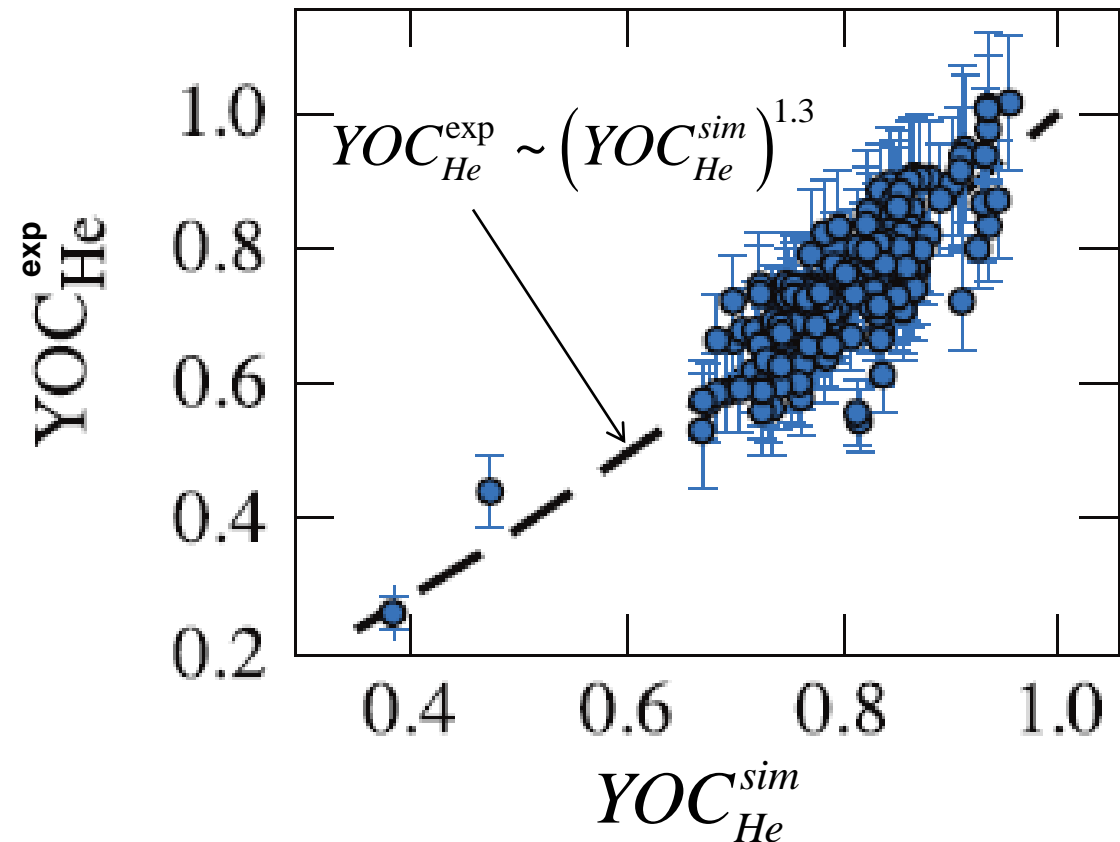
He³ produced from tritium decay accumulates in the DT vapor over time leading to fusion yield degradation

He³ degradation:
simulated dependence from
100% He³ in vapor

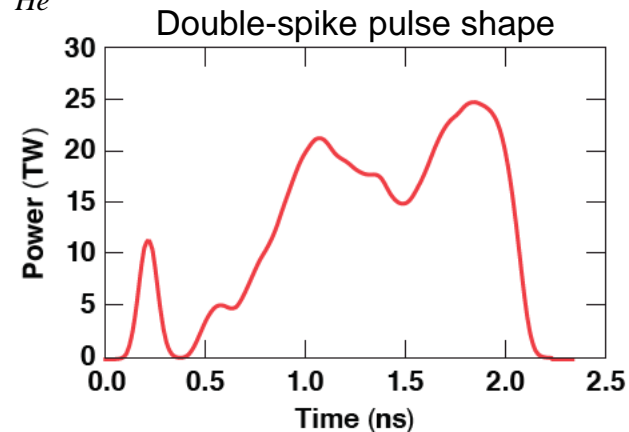
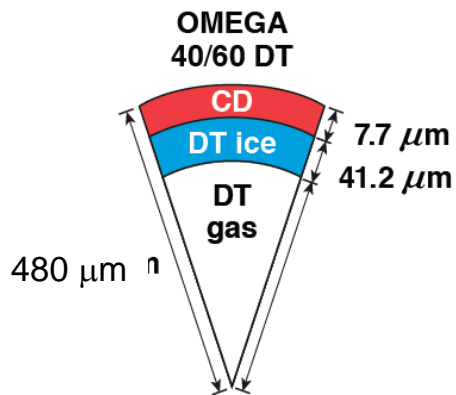
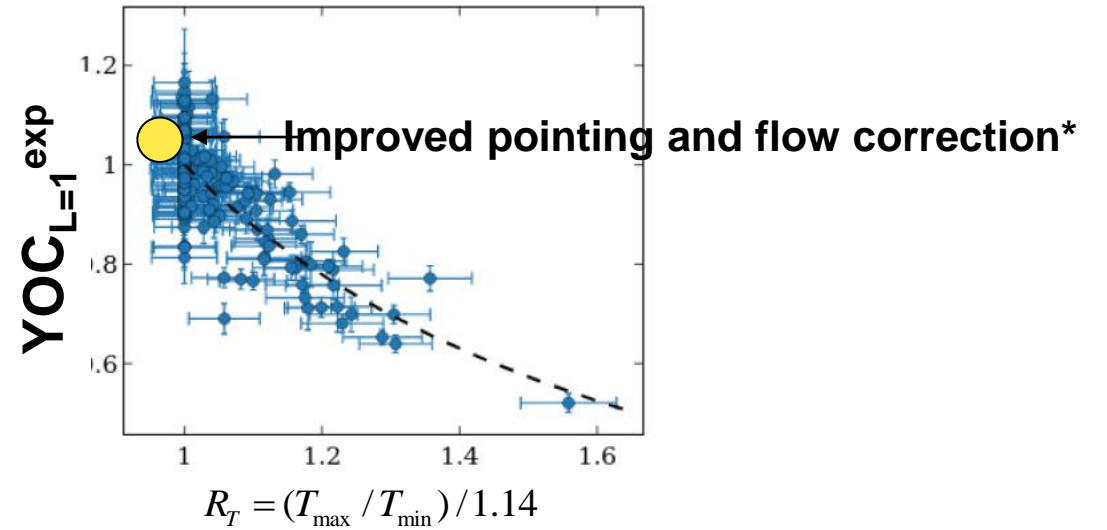
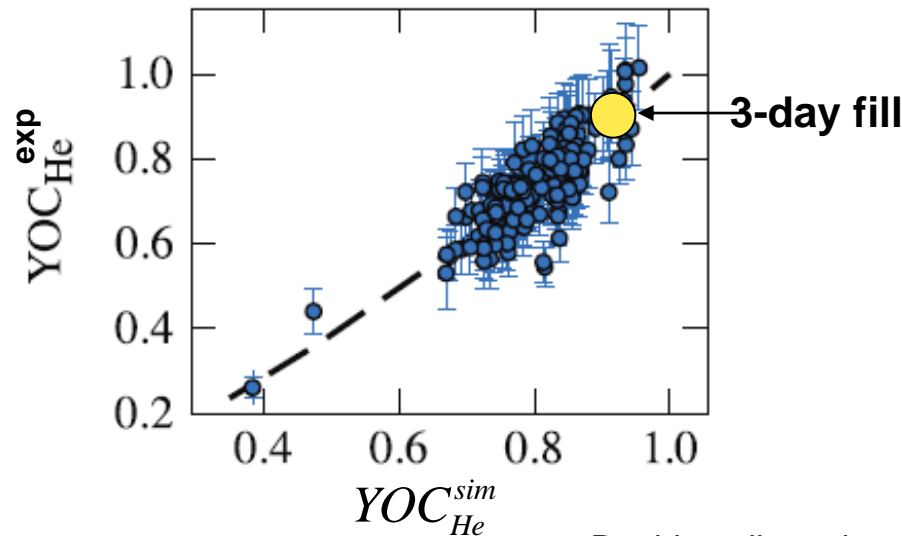


TC15571a

He³ degradation:
experimental dependence



Implosions were optimized with respect to: pulse shaping, He³ accumulation and L=1 suppression using target offsets to compensate for laser mispointing

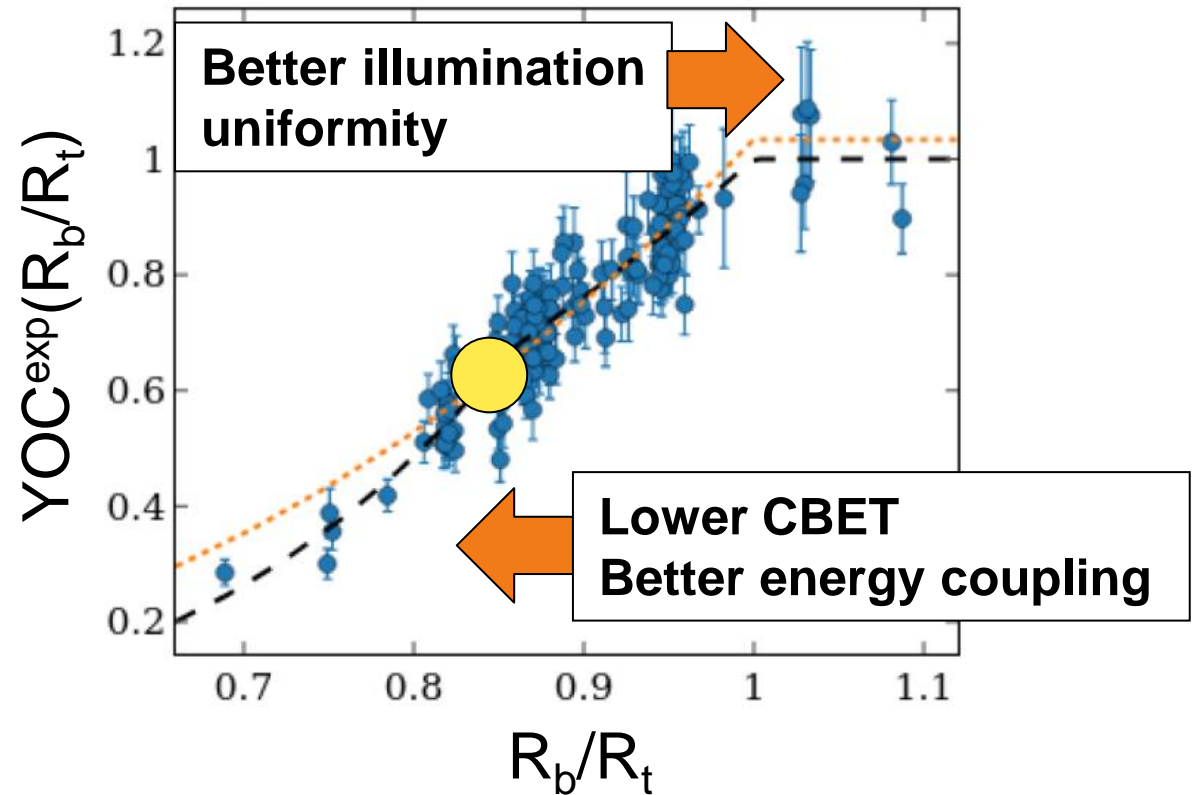
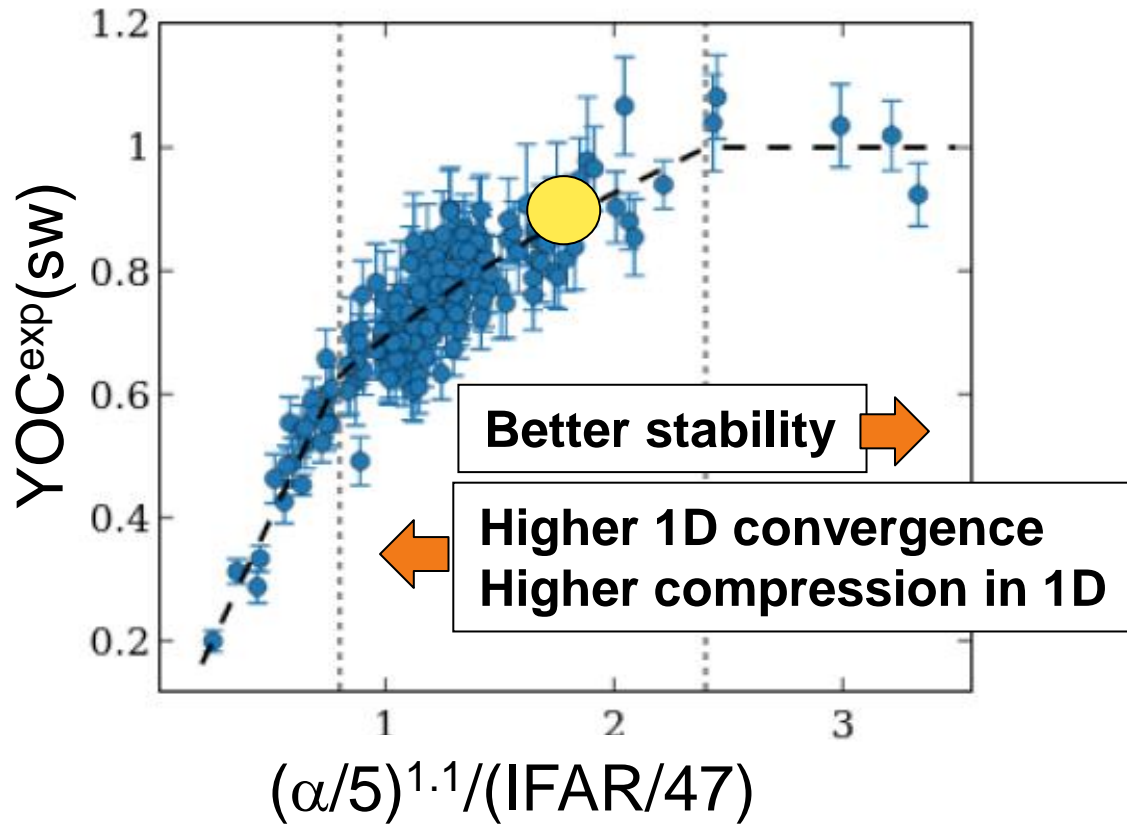


Shot 99922, 90288
 Yield = 1.57e14
 $\rho R = 160 \text{ mg/cm}^2$
 $\chi(2\text{MJ}) \approx 0.74$

*O. Mannion, PoP (2021)

Implosions were also optimized with respect to: hydrodynamic stability, 1D performance, laser beam mode degradation and CBET reduction

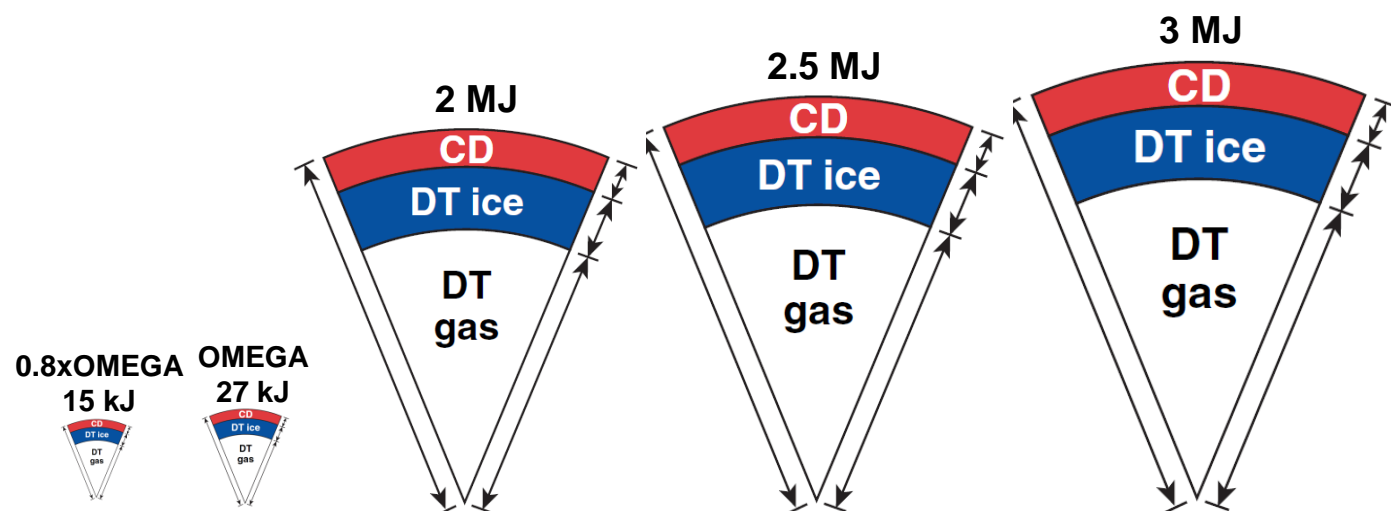
● → optimum



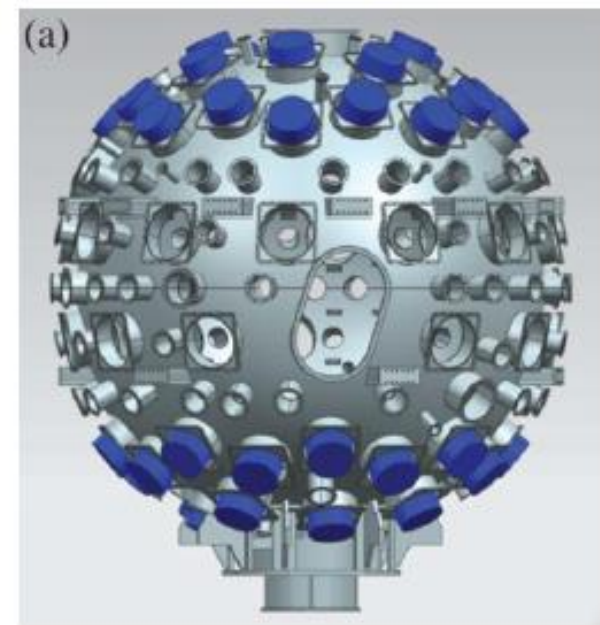
Hydrodynamic scaling does not include important physics such as laser-plasma interactions and the NIF polar geometry

$V_{\text{imp}} = \text{constant}$, Pressure = constant, $\alpha = \text{constant}$

$E_{\text{Laser}} \sim R^3$ Power_{Laser} $\sim R^2$ Mass $\sim R^3$



NIF beam port configuration



Degradation mechanisms affecting the fusion yield of OMEGA implosions have been quantified through statistical mapping to the experimental data

Yield degradation → $YOC = \text{Yield-Over-Clean} = \frac{\text{Yield (measured)}}{\text{Yield (1D codes)}}$

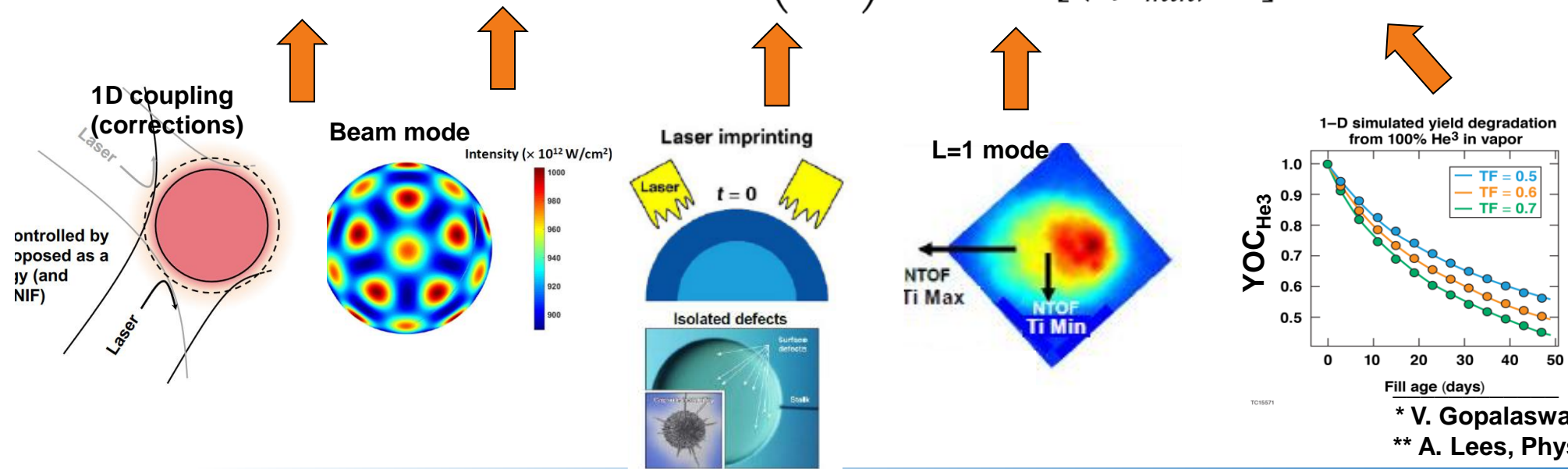
CBET/1D physics?

Beam mode

Short wavelengths $\ell=1$

T-decay

$$YOC \sim \left(\frac{Rb}{Rt}\right)^{b_1} e^{-(b_2 + b_3\alpha + b_4CR)} \sigma_{rms}^{b_5} \left(\frac{\alpha_F^{b_6}}{IFAR}\right)^{b_7, b_8} \text{Max} \left[\left(\frac{T_{max}}{b_9 T_{min}}\right), 1 \right]^{b_{10}} YOC_{He3}^{b_{11}} YOC_{res}$$



* V. Gopalswamy, Nature 565, 581–586 (2019)

** A. Lees, Phys. Rev. Lett.127, 105001 (2021)

The result of the mapping provides individual dependencies¹ of each degradation mechanism and an accurate predictive tool

$$YOC_{exp} = \text{Yield-Over-Clean} = \frac{\text{Yield (measured)}}{\text{Yield (1D codes)}}$$

Short wavelength stability

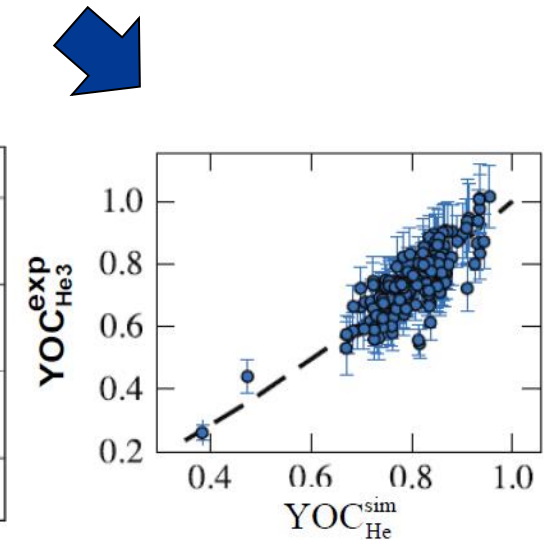
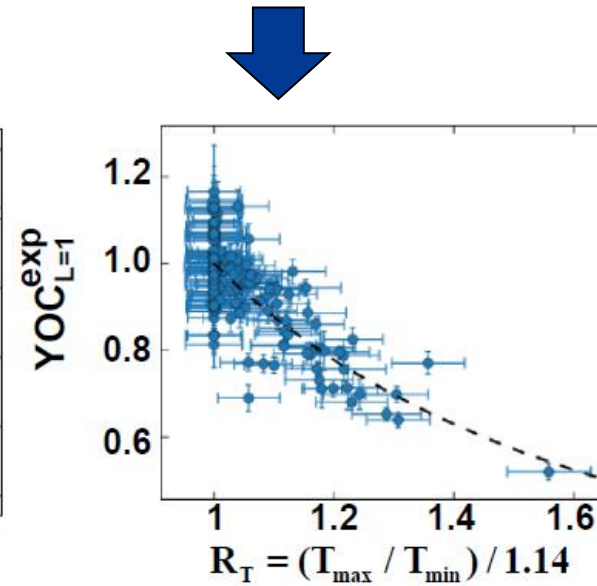
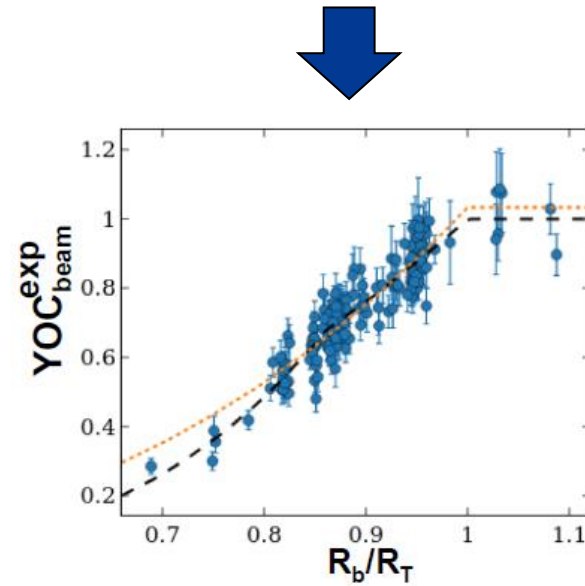
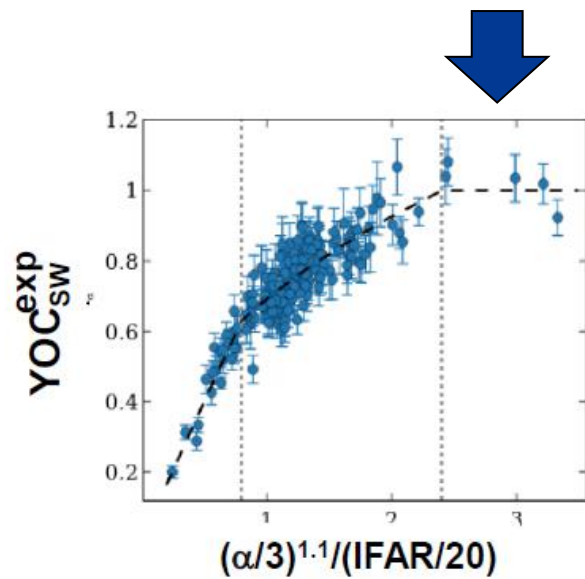
Beam mode + energetics

Beam mode

Mode 1

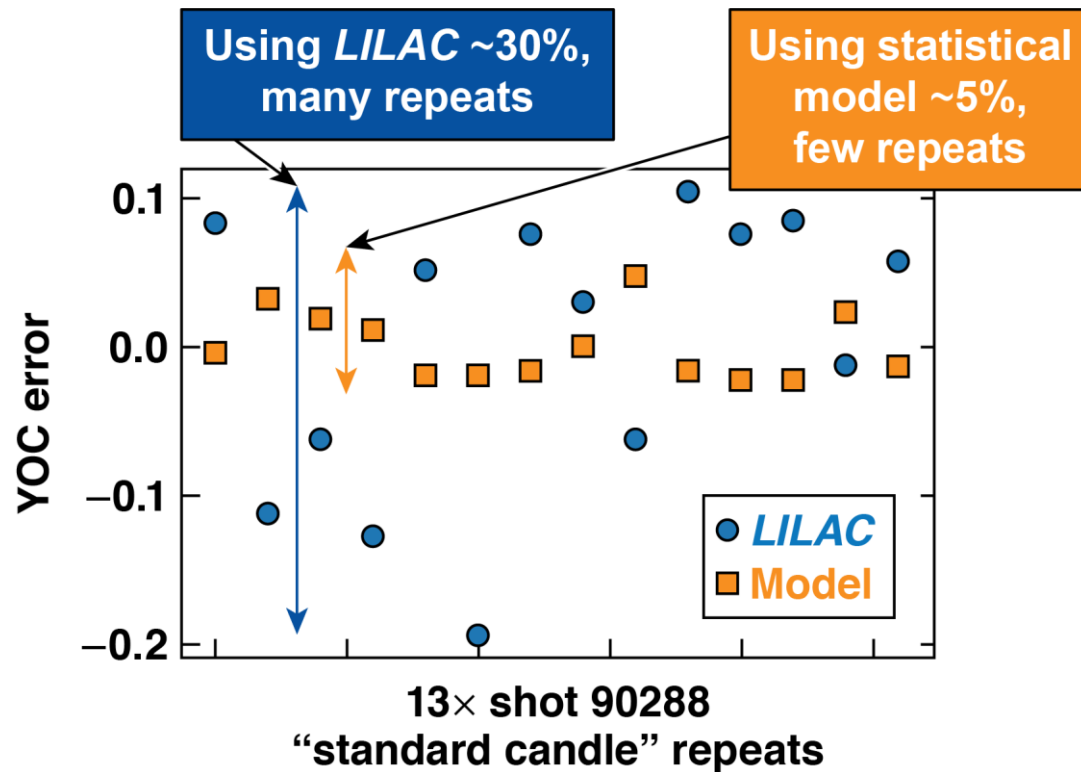
Fill Age

$$YOC_{exp} \sim \left(\frac{(\alpha / 5)^{1.3}}{(IFAR / 47)} \right)^{0.4-0.85} \left(\frac{R_b / R_t}{0.86} \right)^{2.3-4.2} \frac{1}{CR^{0.7}} \left(\frac{T_{min}}{T_{max}} \right)^{1.4} \left(YOC_{He3}^{LILAC} \right)^{1.2}$$

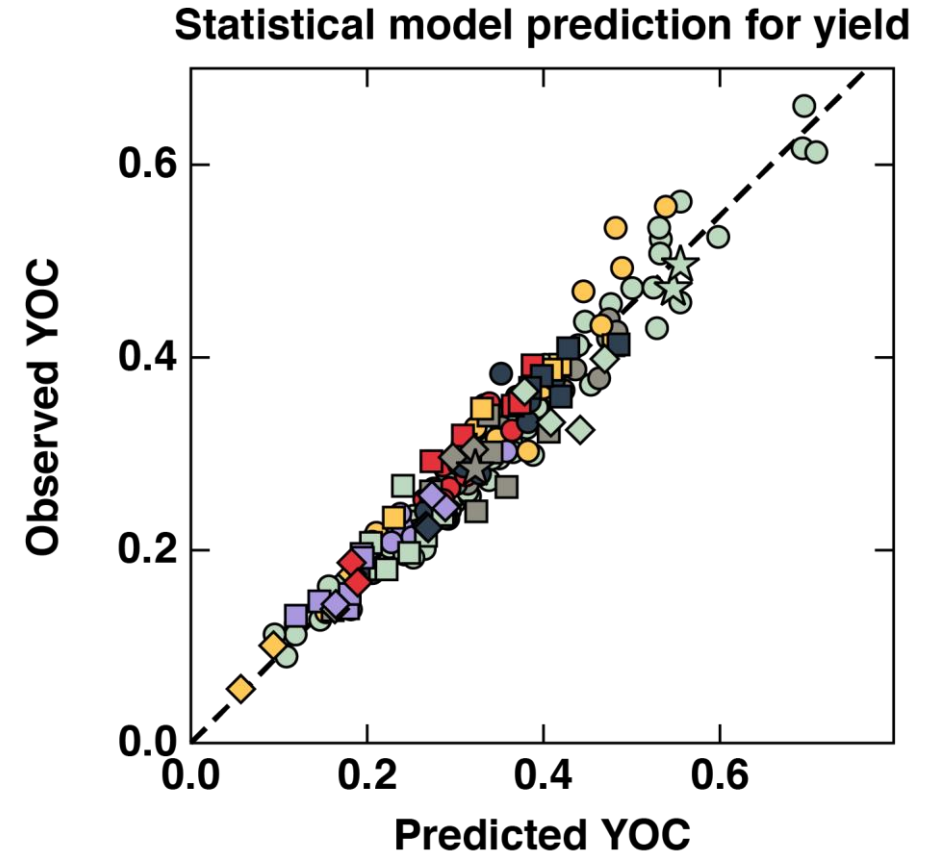


[1] A. Lees et al, PRL (2021), PoP (2023)

Predictive statistical models of the neutron yield are extremely accurate and speed up validation of new designs



TC15878b



TC15878